AFRL-RH-FS-TR-2022-0019

Human Laser Skin Dose-Response Model, Version 2

Elharith Ahmed
Edward A. Early
Brian J. Lund
SAIC

Chad A. Oian
Semih S. Kumru
Robert J. Thomas
711th Human Performance Wing
Airman Systems Directorate
Bioeffects Division
Optical Radiation Bioeffects Branch

December 2022

Interim Report for January 2019 – December 2022

Distribution Statement A: Approved for public release; distribution is unlimited. The views expressed are those of the author and do not necessarily reflect the official policy or position of the Department of the Air Force, the Department of Defense, or the U.S. government.

Air Force Research Laboratory
711th Human Performance Wing
Airman Systems Directorate
Bioeffects Division Optical Radiation Bioeffects Branch
JBSA Fort Sam Houston, Texas 78234

NOTICE AND SIGNATURE PAGE

"Human Laser Skin Dose-Response Model, Version 2 "

(AFRL-RH-FS-TR- 2022- 0019) has been reviewed and is approved for publication in accordance with assigned distribution statement.

FERRIS.LYNDSEY.MARIE.1381070391 Digitally signed by FERRIS.LYNDSEY.MARIE.1381070391 Date: 2022.12.12 16:09:07 -06'00'

LYNDSEY M. FERRIS, LtCol, USAF, BSC
Chief, Optical Radiation Bioeffects Branch

MILLER.STEPHANIE.A.1230536283 Digitally signed by MILLER.STEPHANIE.A.1230536283 Date: 2023.01.29 09:21:03 -06'00'

STEPHANIE A. MILLER, DR-IV, DAF
Chief, Bioeffects Division
Airman Systems Directorate
711th Human Performance Wing
Air Force Research Laboratory

REPORT DOCUMENTATION PAGE

Form Approved
OMB No. 0704-0188

1. REPORT DATE *(DD-MM-YYYY)* 08-DEC-2022

2. REPORT TYPE Interim Technical Report

3. DATES COVERED *(From - To)* Jan 2019 – Dec 2022

4. TITLE AND SUBTITLE
Human Laser Skin Dose-Response Model, Version 2

5a. CONTRACT NUMBER FA8650-19-C-6024

5b. GRANT NUMBER

5c. PROGRAM ELEMENT NUMBER

6. AUTHOR(S)
Elharith Ahmed, Edward Early, Brian Lund, Chad Oian, Semih Kumru, Robert J. Thomas

5d. PROJECT NUMBER

5e. TASK NUMBER

5f. WORK UNIT NUMBER H10G

7. PERFORMING ORGANIZATION NAME(S) AND ADDRESS(ES)
SAIC
4141 Petroleum Rd
JBSA, Fort Sam Houston, Texas 78234

8. PERFORMING ORGANIZATION REPORT

9. SPONSORING / MONITORING AGENCY NAME(S) AND ADDRESS(ES)
711th Human Performance Wing
Airman Systems Directorate
Bioeffects Division
Optical Radiation Branch
JBSA, Fort Sam Houston, Texas 78234

10. SPONSOR/MONITOR'S ACRONYM(S) 711 HPW/RHDO

11. SPONSOR/MONITOR'S REPORT NUMBER(S) AFRL-RH-FS-TR-2022-0019

12. DISTRIBUTION / AVAILABILITY STATEMENT

Distribution A. Approved for public release; distribution is unlimited. CLEARED: PA CASE # AFRL-2023-0511. The opinion expressed on this document, electronic or otherwise, are solely those of the authors. They do not represent an endorsement by or the views of the United States Air Force, the Department of Defense, or the United States Government.

13. SUPPLEMENTARY NOTES

14. ABSTRACT
The increased use of lasers in outdoor, uncontrolled environments requires a generalized human dose-response model for skin injuries to achieve improved fidelity for risk assessment. Experimental data and simulation results are the basis for the developed model, which includes effects from pain to minimal visible lesions to 3rd-degree burns. The model covers the spectral range from 400 nm to 2000 nm and the temporal range from 1 μs to 10 s. Construction of the model captures the essential bio-physical features contributing to human susceptibility to laser injury of the skin, including variability between humans and the effect of the angle of incidence.

15. SUBJECT TERMS

16. SECURITY CLASSIFICATION OF: Unclassified			17. LIMITATION OF ABSTRACT	18. NUMBER OF PAGES	19a. NAME OF RESPONSIBLE PERSON
a. REPORT	**b. ABSTRACT**	**c. THIS PAGE**			Chad Oian
U	U	U	SAR	51	**19b. TELEPHONE NUMBER *(include area code)*** 210-539-8292

Standard Form 298 (Rev. 8-98)
Prescribed by ANSI Std. 239.18

THIS PAGE INTENTIONALLY LEFT BLANK

Table of Contents

SectionPage

LIST OF FIGURES

Page

LIST OF TABLES

Page

1.0 INTRODUCTION

The increased use of lasers in outdoor environments is driving the need for a risk-based approach for laser hazard analyses. For indoor environments, safety with no possibility of injury is the criterion for the analysis; however, for outdoor environments, risk is the more appropriate criterion. While there is a finite probability of injury, this probability needs to be estimated and within an acceptable range. The transition to a risk-based approach to laser hazard analyses requires improved fidelity in models used to assess the risk.

An important model in such a risk-based approach is the probability of skin injury resulting from a laser exposure, quantified by a dose-response model. This model uses a cumulative log-normal distribution to calculate the probability of injury for a given dose. A log-normal distribution has two parameters – the mean and the standard deviation. The mean is the dose that results in a 50 % probability of injury, while the standard deviation quantifies the width of the distribution. The mean effective dose spans effects from sub-threshold (pain) to threshold (minimum visible lesion) to supra-threshold (2^{nd}- and 3^{rd}-degree burns) and the standard deviation accounts for variability between humans and uncertainties in the model. For laser hazards, these parameters are functions of wavelength, exposure duration, and effect.

The following begins with an overview of the dose-response model, including the components of the model. Subsequent sections derive and discuss the three components of the model: 1) a new ED_{50} model for the skin developed from porcine experimental data, 2) a model for the slope resulting from human variability and uncertainties, and 3) a model for effect from the angle of incidence. The first two components address the mean and standard deviation, respectively, required for a log-normal dose-response model. The third component addresses the reduced dose resulting from the angle of incidence. The next two sections detail calculation of the effective dose and a probability of injury, followed by a section applying the model to an example. The final section provides a summary of the human skin dose-response model.

The significant changes from the previous version of this technical report [1] are: removing the explicit dependence on beam diameter by averaging the radiant exposure over the limiting aperture; including sub-threshold effects of sensation and pain; and updating the burn degree types to current descriptions and definitions.

2.0 DOSE-RESPONSE MODEL OVERVIEW

The dose in a dose-response model is typically termed the effective dose with symbol ED. For skin, ED is a radiant exposure with units J/cm^2. The effective dose for which there is a 50 % probability of injury is termed ED_{50}. Similarly, the effective doses for 16 % and 84 % probabilities of injury are termed ED_{16} and ED_{84}, respectively. The slope S is

$$S = \frac{ED_{84}}{ED_{50}} \quad \text{or} \quad S = \frac{ED_{50}}{ED_{16}} \tag{1}$$

The output of the dose-response model is the probability of injury P, given by the cumulative log-normal distribution

$$P(q) = \frac{1}{\sqrt{2\pi\sigma^2}} \int_{-\infty}^{q} exp\left[\frac{-(x-\mu)^2}{2\sigma^2}\right] dx = \frac{1}{2}\,\mathrm{erfc}\left[\frac{-(q-\mu)}{\sqrt{2}\sigma}\right] \tag{2}$$

where

$$q = \log_{10}(ED)\,, \tag{3}$$

$$\mu = \log_{10}(ED_{50})\,, \tag{4}$$

$$\sigma = \log_{10}(S)\,. \tag{5}$$

The logic flow of the human laser skin dose-response model is summarized in Fig. 1, which illustrates the components, inputs, and data flow to arrive at a probability of injury using the quantities in Eqs. (3) to (5). The model is a function of inputs of wavelength λ, exposure duration T, $1/e^2$ beam diameter D_2, irradiance E, and burn degree. Note the burn degree also includes sensation and pain. There are two aspects to the complete model, the mean effective dose ED_{50} and the slope S. Both have models that are functions of wavelength, and a function of exposure duration in the case of the mean effective dose. The human laser skin dose-response model covers the wavelength range from 400 nm to 2000 nm.

The ED_{50} model determines the mean effective dose for a minimum visible lesion (MVL) as a function of the exposure conditions, and the ED_{50} Calculation combines this with the burn degree selected to determine the ED_{50}. Likewise, the slope model determines the slope for a MVL as a function of wavelength, and the slope calculation combines this with the burn degree selected to determine the final slope. The effective dose ED is a function of the exposure duration T, the incident irradiance E, and the $1/e^2$ beam diameter D_2. The probability of injury calculation includes a component due to variability in the angle of incidence, which modifies Eq. (2). The output of the model is a probability of injury for a laser exposure to the human skin.

The following sections detail all the modules shown in Fig. 1. The ED_{50}, slope, and angle models capture the essential physical features involved in each, but these individual modules can be refined in the future as more empirical and modeling results are available and included.

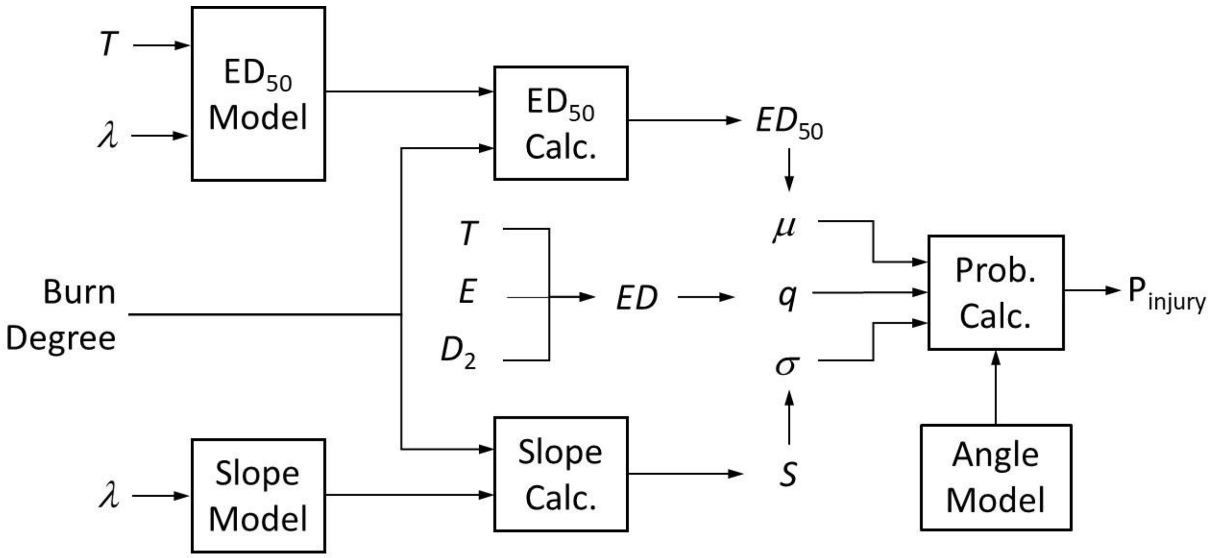

Figure 1. The components of the dose-response model, inputs, and data flow. The components are the ED_{50} and slope, the ED_{50} and slope calculations, and the angle model and probability calculation. The inputs are the wavelength λ, exposure duration T, 1/e^2 beam diameter D_2, irradiance E, and burn degree.

3.0 ED_{50} MODEL

3.1 Introduction

The ED_{50} model is a generalized form for the ED_{50}, also known as the damage threshold, across all applicable wavelengths, exposure durations, and beam diameters. Unlike the case with retina ED_{50} data, the skin ED_{50} data is sparse. For consistency, the sources of data used to model the ED_{50} were further limited to those generated by Air Force Research Laboratory (AFRL) personnel or collaborators [2-6] using Yucatan mini-pigs at near-infrared (NIR) wavelengths (1000 nm to 2000 nm) with a MVL requirement 24 hours after exposure. As will be shown, the ED_{50} model scales the maximum permissible exposure (MPE) in the ANSI Z136.1 American National Standard for Safe Use of Laser [7] across all applicable wavelengths and exposure durations.

Values for skin MPE are defined as the average radiant exposure H over a limiting aperture D_f of 0.35 cm, with units of J/cm^2, for exposure durations less than 10 s [7]. Longer exposure durations have an MPE defined as the average irradiance E. The sources of skin data typically report ED_{50} in terms of energy Q or radiant exposure, and all report spot sizes as 1/e^2 beam diameters D_2. Appendix A provides the reported ED_{50} values for all sources of data used in the following, along with the calculated average radiant exposure.

For Gaussian beams, the peak radiant exposure H_{peak} is

$$H_{\text{peak}} = \frac{8}{\pi}\frac{Q}{D_2^2} \ , \tag{6}$$

and the average radiant exposure H_{avg} over the limiting aperture is

$$H_{\text{avg}} = \frac{H_{\text{peak}}}{2}\left(\frac{D_2}{D_{\text{f}}}\right)^2 \left\{1 - \exp\left[-2\left(\frac{D_{\text{f}}}{D_2}\right)^2\right]\right\} \ . \tag{7}$$

For flat-top beams with diameter D,

$$H_{\text{peak}} = H_{\text{avg}} = \frac{4}{\pi}\frac{Q}{D^2} \ . \tag{8}$$

Radiant exposure in terms of irradiance is

$$H = E \cdot T \ , \tag{9}$$

and energy in terms of power Φ is

$$Q = \Phi \cdot T \ , \tag{10}$$

where T is the exposure duration.

3.2 Exposure Duration Dependence

The ANSI Z136.1 standard MPE has a $T^{1/4}$ exposure duration dependence [7]. The experimental data have a similar trend with exposure duration, as shown in Fig. 2. Therefore, a $T^{1/4}$ exposure duration dependence for the ED_{50}, based on the MPE trend, is reasonable.

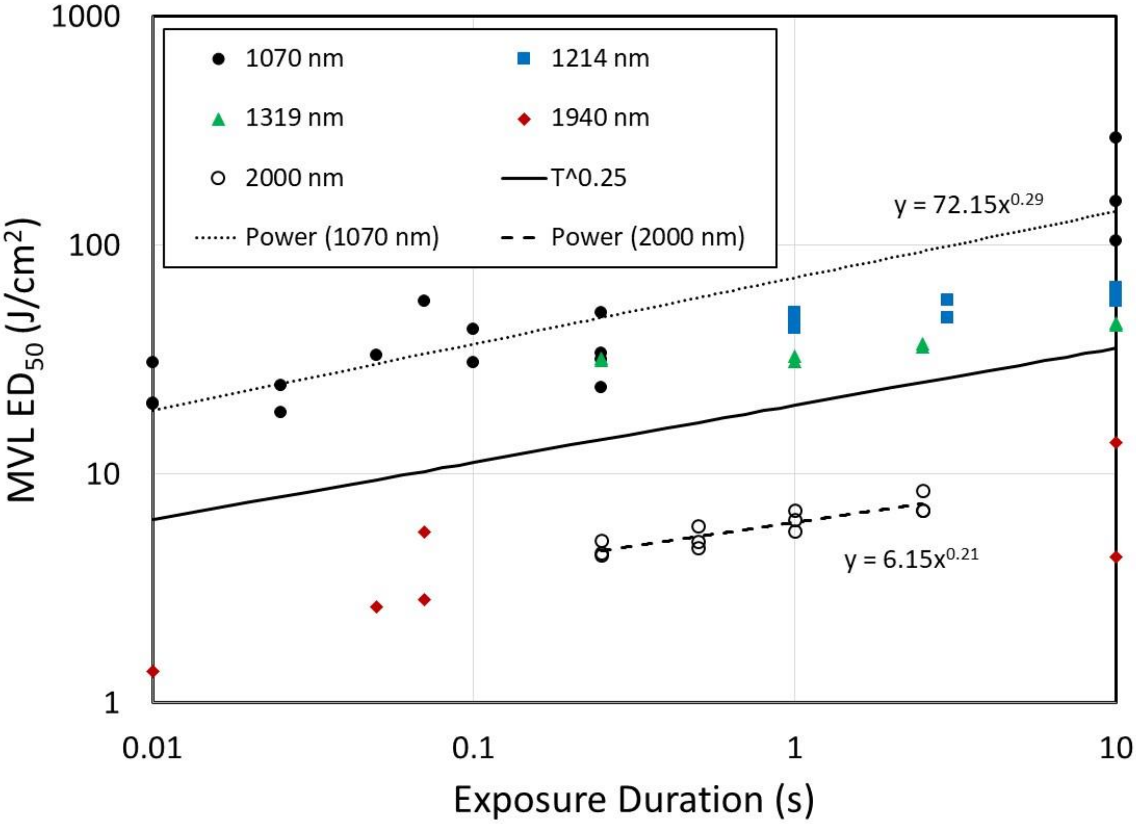

Figure 2. Exposure duration dependence of the ED_{50} from experimental data. Fits to a power law are shown for selected wavelengths and for the $T^{1/4}$ dependence.

3.3 Beam Diameter Dependence

The experimental data, with ED_{50} expressed as the average radiant exposure over the limiting aperture, has an inconclusive dependence on beam diameter. There should be no dependence on beam diameter for short exposure durations, while longer exposure durations should show a decrease with increasing beam diameter as thermal diffusion and boundary losses become relevant. Results from the Scalable Effects Simulation Environment (SESE) support this trend with exposure duration. SESE is a computer program that models the thermal response of tissue to incident laser radiation by performing time-dependent simulations in a three-dimensional spatial domain [8]. The relevant physical, optical, and thermal properties of the skin tissue layers required as inputs to SESE are listed in Table 1. Threshold radiant exposures for 1st-degree burns as a function of beam diameter are shown in Fig. 3 for exposure durations of 0.1 s and 2 s. As postulated, the longer exposure duration has a greater dependence on beam diameter than does the shorter exposure duration.

Table 1. Skin tissue layer optical and thermal properties.

Property	Epidermis	Dermis	Fat
Thickness (mm)	0.082	2.7	15
Optical Absorption Coefficient (1/m)	35	17	103
Reduced Scattering Coefficient (1/m)	1740	1540	894
Water Fraction	0.3	0.8	0.2
Density (kg/m^3)	1210	1060	850
Specific Heat (J/(kg K))	2244	3663	2070
Thermal Conductivity (W/(m K))	0.20	0.49	0.16
Blood Perfusion Rate (1/s)	0	1.25 x 10^{-3}	1.25 x 10^{-3}

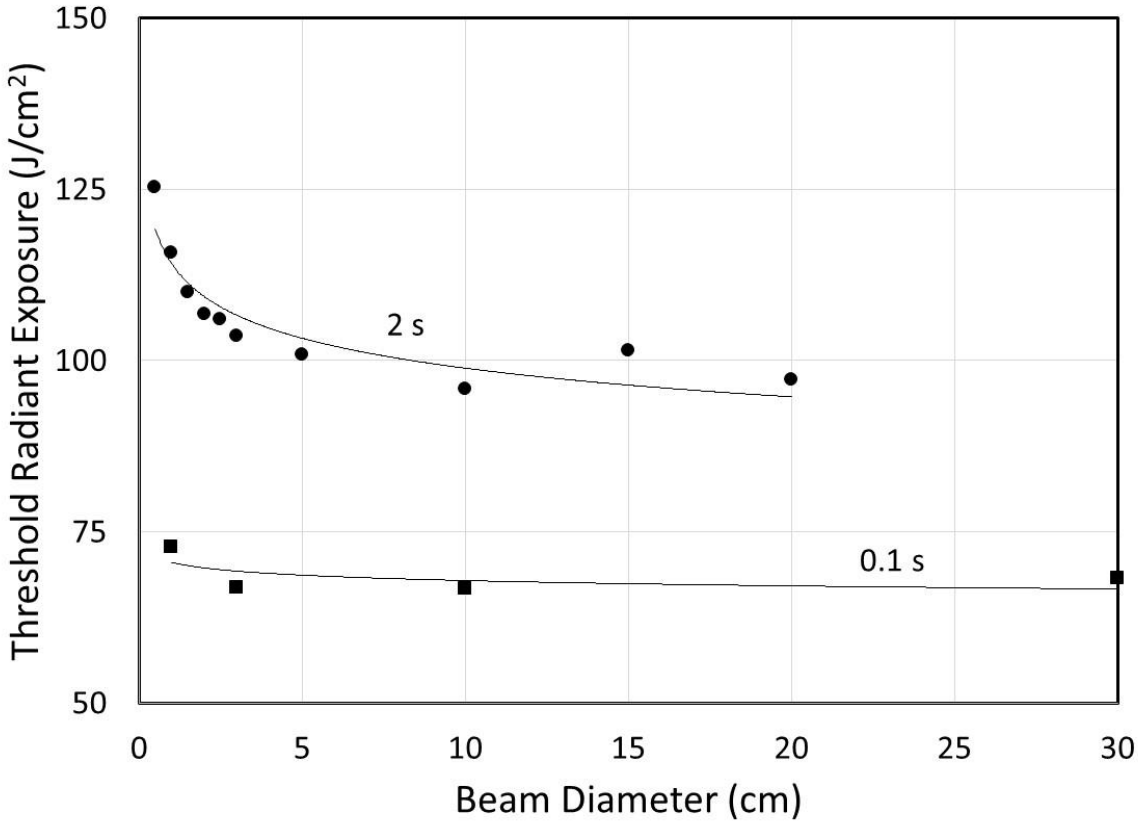

Figure 3. Simulated threshold radiant exposures for 1st-degree burns as a function of beam diameter for the indicated exposure durations, with fits to a power law.

3.4 MVL ED_{50}

The MVL ED_{50} for skin, expressed as the average radiant exposure over the limiting aperture, scales as $T^{1/4}$ for exposure duration, as detailed Section 3.2. The remaining step is to assign a value to the MVL ED_{50} based on the ratio of experimental values to the MPE. The most extensive experimental data was collected at a wavelength of 1070 nm [2]. The ratio of the average radiant exposure to the MPE, over all beam diameters and exposure durations, is provided in Table 2. The average ratio is 12.0 with a standard deviation of 3.76, with the largest ratio of 29.96 excluded.

The ratio at a wavelength of 1070 nm, and other wavelengths [3-6], along with another experiment at 1070 nm [9], are shown in Fig. 4. The ratios at wavelengths of 1214 nm and 1319 nm are significantly less than 12.0, while those at the longer wavelengths of 1940 nm and 2000 nm are in agreement with the ratio at 1070 nm, as is the most-recent data by DeLisi at a wavelength of 1070 nm [9]. Investigations of the origin of the discrepancy at wavelengths in the 1200 nm to 1300 nm range yielded no conclusions, although possibilities are incorrect MPEs or the influence of water content and absorption. The agreement of ratios at wavelengths near 1000 nm and 2000 nm provides confidence in using a value of 12.0 to scale the MPE to the MVL ED_{50}. Since porcine experimental subjects have skin properties comparable to those of humans, there is no adjustment from a non-human to a human ED_{50}, in contrast to the adjustment in the retinal human dose-response model [10].

Table 2. Experimental data at a wavelength of 1070 nm used to scale the MPE to the ED_{50}.

D_2 (cm)	T (s)	H_{avg} (J/cm^2)	MPE (J/cm^2)	H_{avg}/MPE
0.6	0.01	20.5	1.74	11.80
0.6	0.07	57.0	2.83	20.13
0.6	*10*	*293.0*	*9.78*	*29.96*
1.1	0.01	30.7	1.74	17.64
1.1	0.1	43.1	3.09	13.92
1.1	10	156.2	9.78	15.97
1.9	0.05	33.1	2.60	12.74
1.9	0.25	50.6	3.89	13.01
1.9	10	105.0	9.78	10.74
2.4	0.01	20.2	1.74	11.60
2.4	0.025	18.6	2.19	8.51
2.4	0.25	23.9	3.89	6.15
4.7	0.025	24.5	2.19	11.18
4.7	0.1	30.6	3.09	9.90
4.7	0.25	33.8	3.89	8.70
9.5	0.25	31.7	3.89	8.15
			Average	12.0
			Standard Deviation	3.76

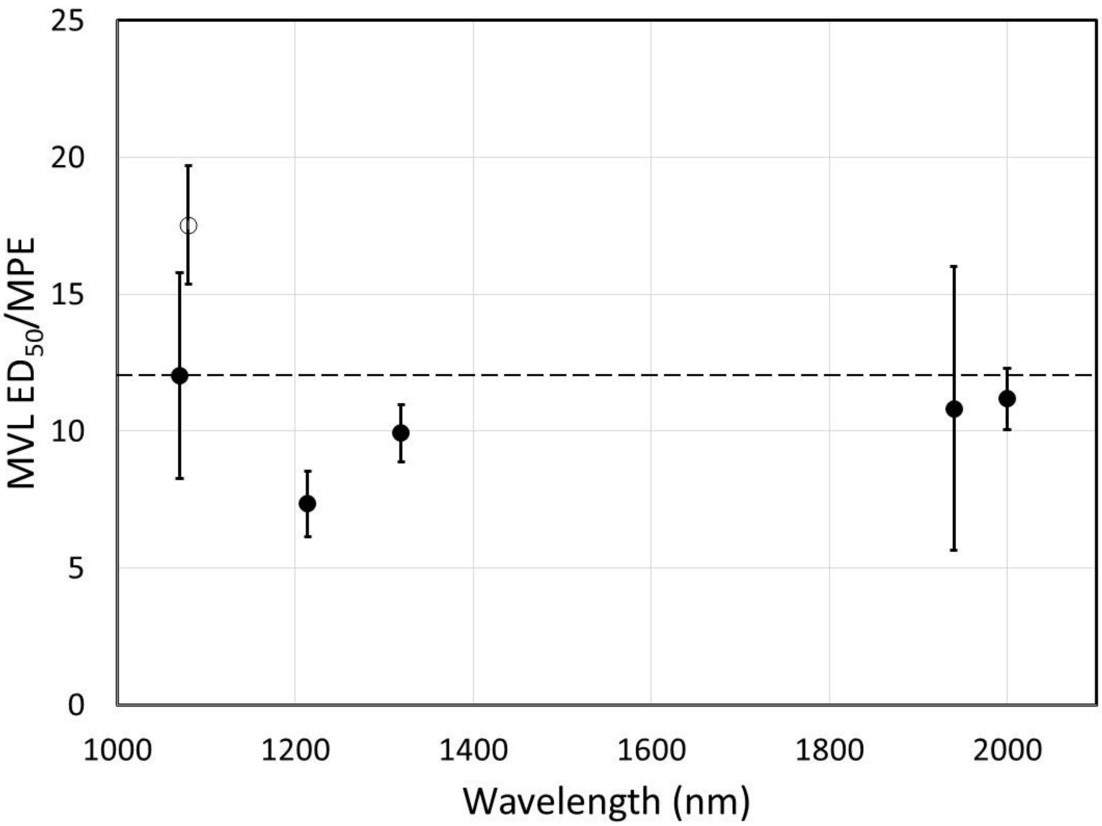

Figure 4. Ratio of experimental *ED*50 to MPE over ranges of exposure duration at each wavelength.

The ED_{50} model for skin MVL is therefore

$$MVL\ ED_{50}(\lambda, T) = 12.0 \times MPE(\lambda, T)\,. \tag{11}$$

The agreement between model and experiment is illustrated in Fig. 5 at a wavelength of 1070 nm as a function of exposure duration. While the Vincelette data [2] was used to determine the ratio of ED_{50} to MPE, the excellent agreement between model and experiment for other sources of data [9, 11, 12] provides high confidence in the model.

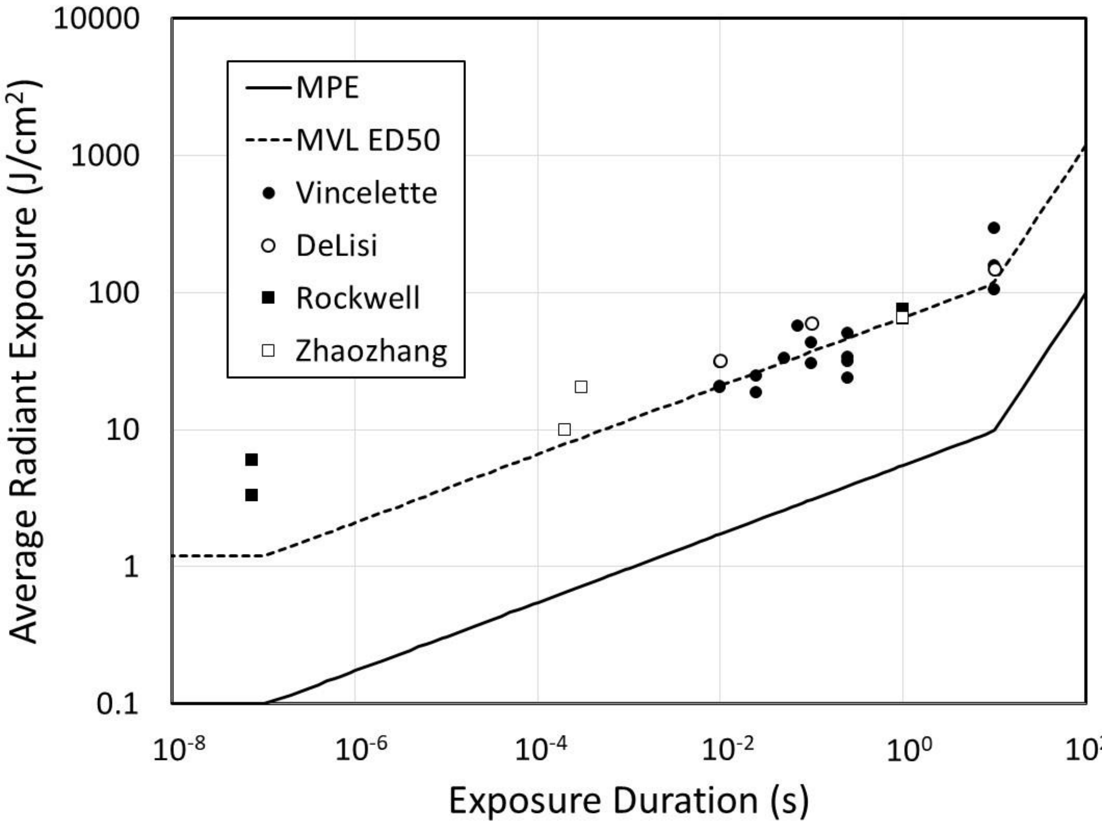

Figure 5. Time dependence of ED_{50} at 1070 nm for experimental data, the MVL ED_{50} model, and the MPE.

3.5 Supra-Threshold ED_{50}

An MVL is equivalent to a first-degree burn. Laser illumination can also cause more severe burns, termed supra-threshold effects [13]. A first-degree burn affects only the epidermis, has redness without blistering, and heals without scarring. Second-degree burns are partial-thickness and divide between superficial and deep. The former affects the epidermis and the papillary layer of the dermis, while the latter affects down to the reticular layer of the dermis. The former has redness with blistering and heals without scarring, while the latter is pale with blistering and scars upon healing. A third-degree burn is full-thickness, affects the entire epidermis and dermis layers, has a white to black appearance, and heals with significant scarring.

The Arrhenius damage integral Ω quantifies damage in simulations, with $\Omega = 1$ signifying irreversible damage [14, 15]. The SESE simulation determined threshold powers for each burn degree, using the criteria in Table 3, for a range of exposure durations and beam diameters. These threshold powers are detailed in Appendix B. The ratios of supra-threshold powers to the power for a 1st-degree burn are shown in Fig. 6 for all simulation conditions. The sections of data correspond to fixed beam diameters, with increasing exposure duration within each section. Fits for averages over diameter as a function of time are shown in Fig. 7 and quantified in Table 4. The standard deviations in Table 4 are those of the differences between simulated and fit ratios.

Table 3. Simulation burn criteria.

Burn	Criteria
1st-Degree	$\Omega = 1$ at top of epidermis
2nd-Degree Superficial	$\Omega = 1$ to top of dermis
2nd-Degree Deep	$\Omega = 1$ to 1/3 of dermis thickness
3rd-Degree	$\Omega = 1$ to bottom of dermis

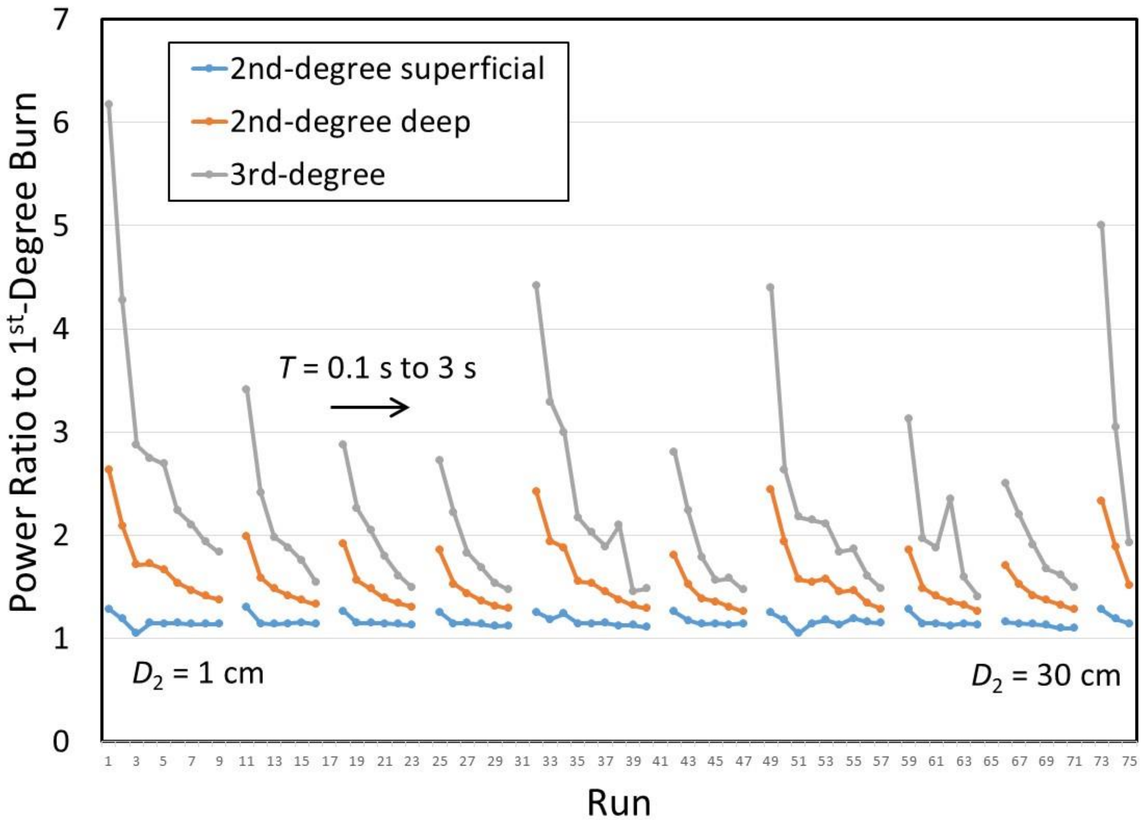

Figure 6. Ratio of burn degree powers to power for 1st-degree burn over ranges of exposure durations and beam diameters.

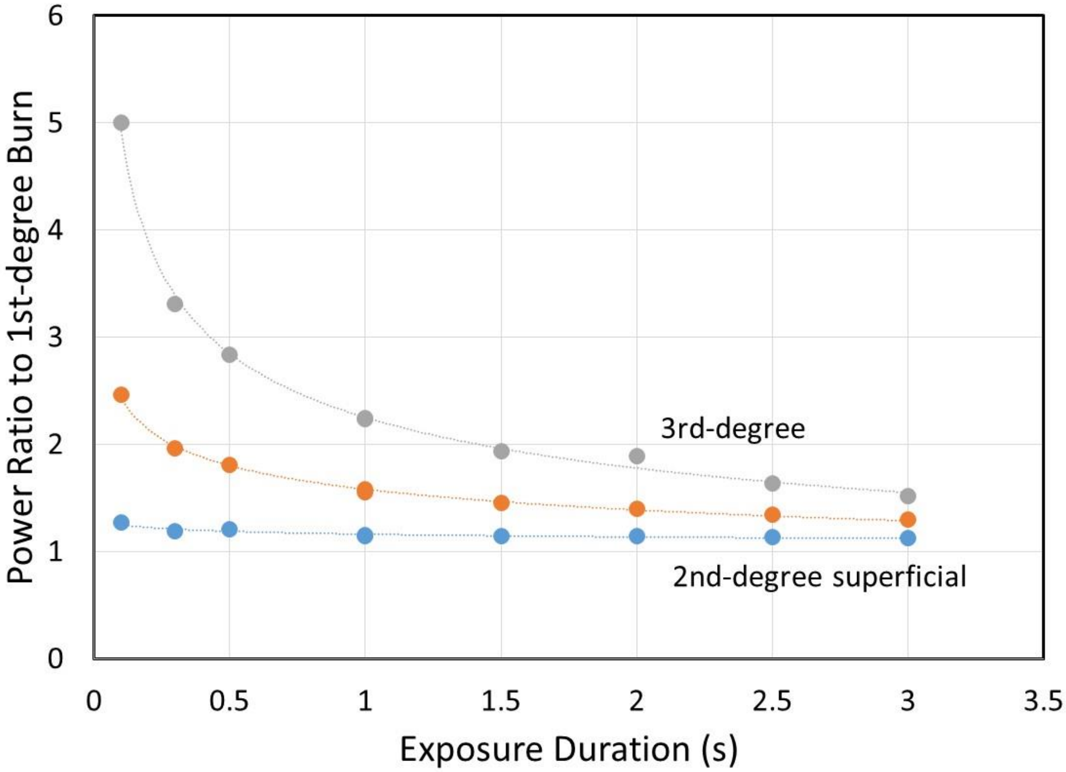

Figure 7. Average ratio of burn degree powers to power for 1st-degree burn over ranges of exposure durations, and power law fits.

Table 4. Supra-threshold ratios for burn severities.

	Supra-threshold Power Ratio to MVL Power	
Burn Severity	Average	Standard Deviation (%)
2nd-superficial	$1.16\ T^{-0.033}$	3
2nd-deep	$1.58\ T^{-0.19}$	4
3rd	$2.25\ T^{-0.34}$	11

The supra-threshold ED_{50} is

$$ED_{50} = \alpha \cdot \text{MVL } ED_{50}, \quad (12)$$

where α corresponds to the average for the supra-threshold burn severity in Table 4.

3.6 Sub-Threshold ED_{50}

Pain precedes injury and elicits an avoidance response. For example, accidentally touching a hot object causes a person to remove their hand automatically and rapidly from the object. Even with this response, a burn can occur. A similar reaction occurs when laser illumination is the source of heat for a burn. The reaction time from onset of pain (when nerve endings in the dermis reach 43 °C) to avoidance movement is at least 100 ms [16] and can be longer. If a person is free to move, this reaction time sets an upper limit on exposure duration. Therefore, the time of onset of pain is important for assessing possible injuries from laser exposure.

Sub-threshold effects are sensation of warmness and pain. The radiant exposures causing these effects are less than that for an MVL, hence the term sub-threshold. Experimental data on sensation and pain is very sparse. Therefore, the goal is to use the available data to scale sub-threshold effects to the MPE, similar to the approach for the MVL threshold. The relevant experimental data for this approach is summarized in Table 5 and detailed in Appendix C.

Table 5. Experimental data sources for indicated thresholds.

				Measured Threshold			
Source	Wavelength	Exposure Duration	Beam Diameter	Sensation	Pain	MVL	2nd-Degree Superficial Burn
Stoll [17, 18]	Broadband	1 s – 35 s	15 mm		X		X
Arendt-Nielson [19]	488 nm, 515 nm, 10.6 μm	50 ms – 500 ms	3 mm	X	X		
Tata [20]	2000 nm	0.25 s – 2.5 s	0.5 cm, 1.5 cm	X		X	
DeLisi [21]	1070 nm	3 ms, 100 ms	3 mm, 7 mm			X	X

The results of Arendt-Nielsen [19] are the model to scale sensation and pain to the other effects of MVL and supra-threshold injuries. Arendt-Nielsen provides power thresholds for sensation and pain at Argon laser wavelengths of 488 nm and 515 nm for a 3 mm uniform beam diameter and exposure durations from 50 ms to 500 ms. These thresholds, with exposure durations in milliseconds, are

$$\Phi(T) = \begin{cases} 50.2\, T^{-0.78}\ \text{W} & \text{Sensation} \\ 64.1\, T^{-0.68}\ \text{W} & \text{Pain} \end{cases} . \tag{13}$$

Converting Eq. (13) to average radiant exposure over the 3 mm beam diameter with exposure duration in seconds yields

$$H(T) = \begin{cases} 3.25\, T^{0.22} \ \ \text{J/cm}^2 & \text{Sensation} \\ 8.27\, T^{0.32} \ \ \text{J/cm}^2 & \text{Pain} \end{cases} . \tag{14}$$

The MPE at visible wavelengths and the exposure durations [7] is 1.1 $T^{0.25}$ J/cm^2. Applying the scaling from MPE to MVL and 2nd-degree superficial burn from Sections 3.4 and 3.5, the average radiant exposure thresholds for these effects are

$$H(T) = \begin{cases} 13.2\, T^{0.25} \ \ \text{J/cm}^2 & \text{MVL} \\ 15.3\, T^{0.217} \ \ \text{J/cm}^2 & 2^{\text{nd}} - \text{degree Superficial} \end{cases} . \tag{15}$$

Stoll [17, 18] provides exposure duration data from 1 s to 35 s for pain and 2nd-degree superficial burns for a broadband source with a 15 mm beam diameter and fixed irradiances. These data, converted to radiant exposure and fit to a power law, are

$$H(T) = \begin{cases} 2.9162\, T^{0.2553} \ \ \text{J/cm}^2 & \text{Pain} \\ 5.4353\, T^{0.2838} \ \ \text{J/cm}^2 & 2^{\text{nd}} - \text{degree Superficial} \end{cases} . \tag{16}$$

Tata [20] provides peak radiant exposure threshold data for both sensation and MVL at a wavelength of 2000 nm for 1/e^2 beam diameters of 0.5 cm and 1.5 cm and exposure durations from 0.25 s to 2.5 s. DeLisi [21] provides peak radiant exposure data for MVL and 2nd-degree superficial burns at a wavelength of 1070 nm for 1/e^2 beam diameters of 3 mm and 7 mm and exposure durations of 3 ms and 100 ms. The resulting average radiant exposures for both data sources are provided in Appendix C.

The supra-threshold effects in Section 3.5 are scaled from the MVL radiant exposure threshold, which in turn is scaled from the MPE. Can sub-threshold effects also be scaled from the MPE? Validating this premise requires comparison of ratios of radiant exposures for the different effects between the model detailed in Eqs. (14) and (15) and experimental data. The sources of data, exposure durations, and radiant exposures for this comparison are given in Table 6, along with the corresponding ratios of radiant exposures. Ratios are the appropriate quantity for comparison because of the different wavelengths involved. The good agreement between ratios for each set of experimental data, with individual ratios within 10 % of the average over both, validates the scaling of sub-threshold effects from the MPE.

Table 6. Radiant exposures and ratios for comparison of sub-threshold model with experimental data.

	Source					
	Stoll	Model	Tata	Model	DeLisi	Model
	Exposure Duration (ms)					
	250		250		100	
Effect	Radiant Exposure (J/cm^2)					
Sensation	-----	-----	1.027	2.40	-----	-----
Pain	2.05	5.31	-----	-----	-----	-----
MVL	-----	-----	4.53	9.33	150.3	7.42
2nd-Degree Superficial	3.67	11.3	-----	-----	221.9	9.28
Ratios						
2nd-Degree / Pain	1.8	2.1	-----	-----	-----	-----
MVL / Sensation	-----	-----	4.4	3.9	-----	-----
2nd-Degree / MVL	-----	-----	-----	-----	1.5	1.3

Applying the entire range of scaling to a wavelength of 1070 nm yields the following ED_{50} radiant exposure thresholds, which are also illustrated in Fig. 8. For sub-threshold effects, Eq. (14) is multiplied by the ratio of the MPE at 1070 nm to that at visible wavelengths, yielding

$$ED_{50}(T) = \begin{cases} 16.3\,T^{0.22}\ \text{J/cm}^2 & \text{Sensation} \\ 41.4\,T^{0.32}\ \text{J/cm}^2 & \text{Pain} \end{cases} . \tag{17}$$

For the MVL, which is equivalent to a 1st-degree burn,

$$ED_{50}(T) = 66\,T^{0.25}\ \text{J/cm}^2 . \tag{18}$$

For supra-threshold effects,

$$ED_{50}(T) = \begin{cases} 76.6\,T^{0.22}\ \text{J/cm}^2 & \text{2nd}-\text{degree Superficial} \\ 104.3\,T^{0.06}\ \text{J/cm}^2 & \text{2nd}-\text{degree Deep} \\ 148.5\,T^{-0.09}\ \text{J/cm}^2 & \text{3rd}-\text{degree} \end{cases} . \tag{19}$$

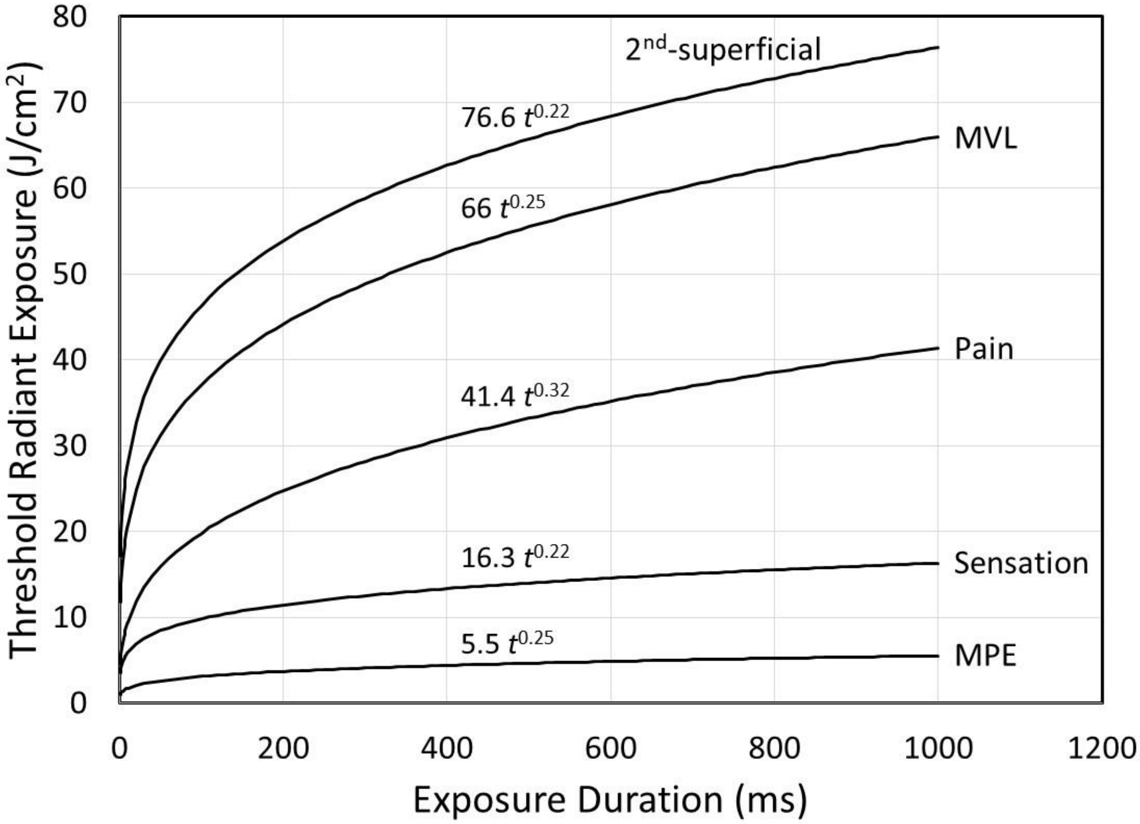

Figure 8. ***ED_{50}*** **threshold radiant exposures for indicated effects from MPE to 2nd-degree superficial burn.**

4.0 SLOPE MODEL

Skin susceptibility to laser damage is a bio-physical process, so variability among humans contributes to the slope model. The human population has a range of skin pigmentation density, but the amount of pigment does not always directly relate to susceptibility. Skin contains multiple chromophores such as melanin, hemoglobin, water, and fat. The concentration of melanin determines skin color, with very low concentrations for light complexioned Caucasian skin (Type I) to high concentrations for black African skin (Type IV) [22]. The other chromophores also contribute to susceptibility and attempts to model human variability based on absorption by these chromophores were unsuccessful. The approach by Jacques [23] resulted in excessive variability at short wavelengths due to melanin content, and suffered from complexity and insufficient data, so was not pursued further.

Fortunately, the spectrophotometry group at the National Institute of Standards and Technology (NIST) recently measured and reported the spectral reflectance $\rho(\lambda)$ of human skin for 100 participants in the study [24]. The range of skin spectral reflectance is shown in Fig. 9, where there is obviously greater variability at wavelengths less than 1000 nm than at longer wavelengths. Also, note the decrease in variability at the shortest wavelengths, in contrast to expectations based on only melanin concentration, which should have greatest variability at these wavelengths. Since thermal damage is proportional to the energy absorbed by the skin, the important quantity is the spectral absorptance $\alpha(\lambda)$,

$$\alpha(\lambda) = 1 - \rho(\lambda). \tag{20}$$

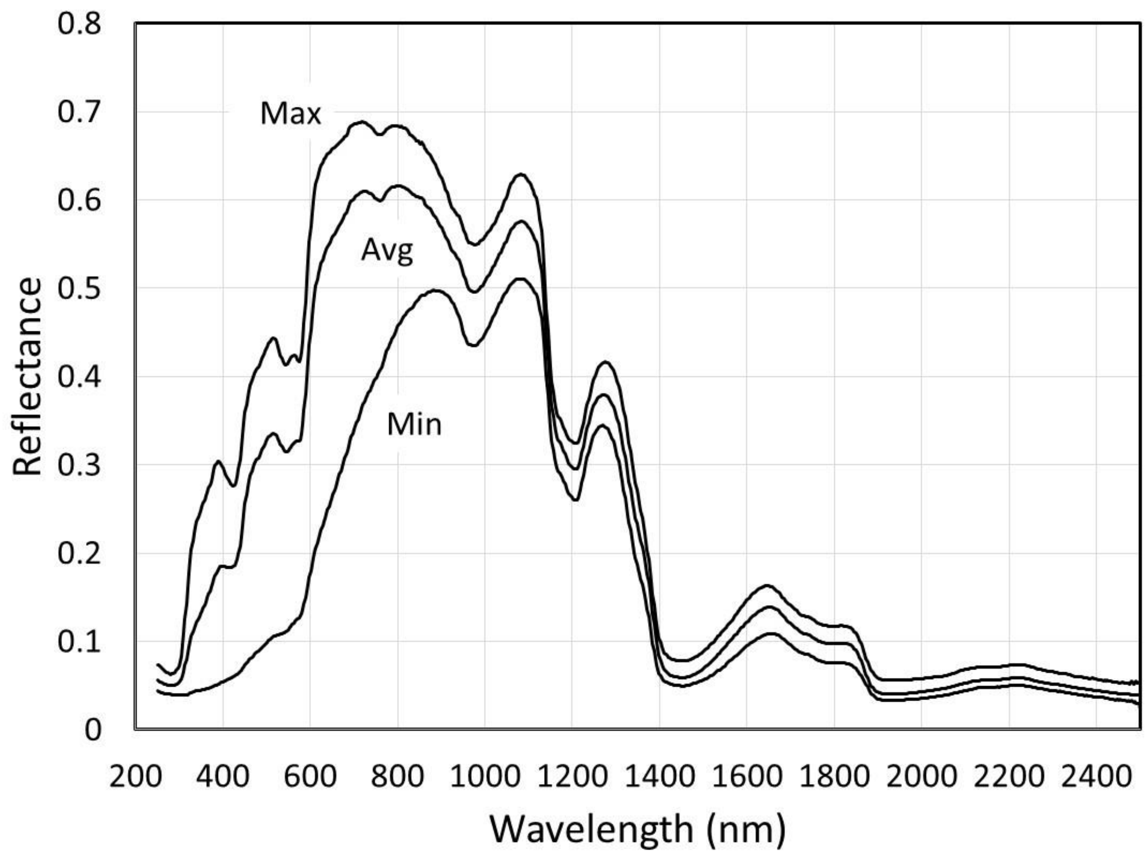

Figure 9. Spectral reflectance of human skin from NIST data.

The human skin reflectance data [24] did not include information on skin color or demographics. Therefore, the maximum and minimum values of absorptance at each wavelength are assumed to be one-standard deviation values of a Gaussian distribution. Using Eq. (1), the slope *S* is therefore

$$S = \frac{\alpha_{max}}{\alpha_{mean}} \ or \ S = \frac{\alpha_{mean}}{\alpha_{min}}. \tag{21}$$

Taking the geometrical mean yields the slope S_A due to variability in human skin absorptance,

$$S_A(\lambda) = \sqrt{\frac{\alpha_{max}(\lambda)}{\alpha_{min}(\lambda)}}. \tag{22}$$

The maximum and minimum spectral absorptance of human skin using the NIST data is listed in Appendix D, and the resulting standard deviation σ_A is shown in Fig. 10. Variability is greatest at visible wavelengths.

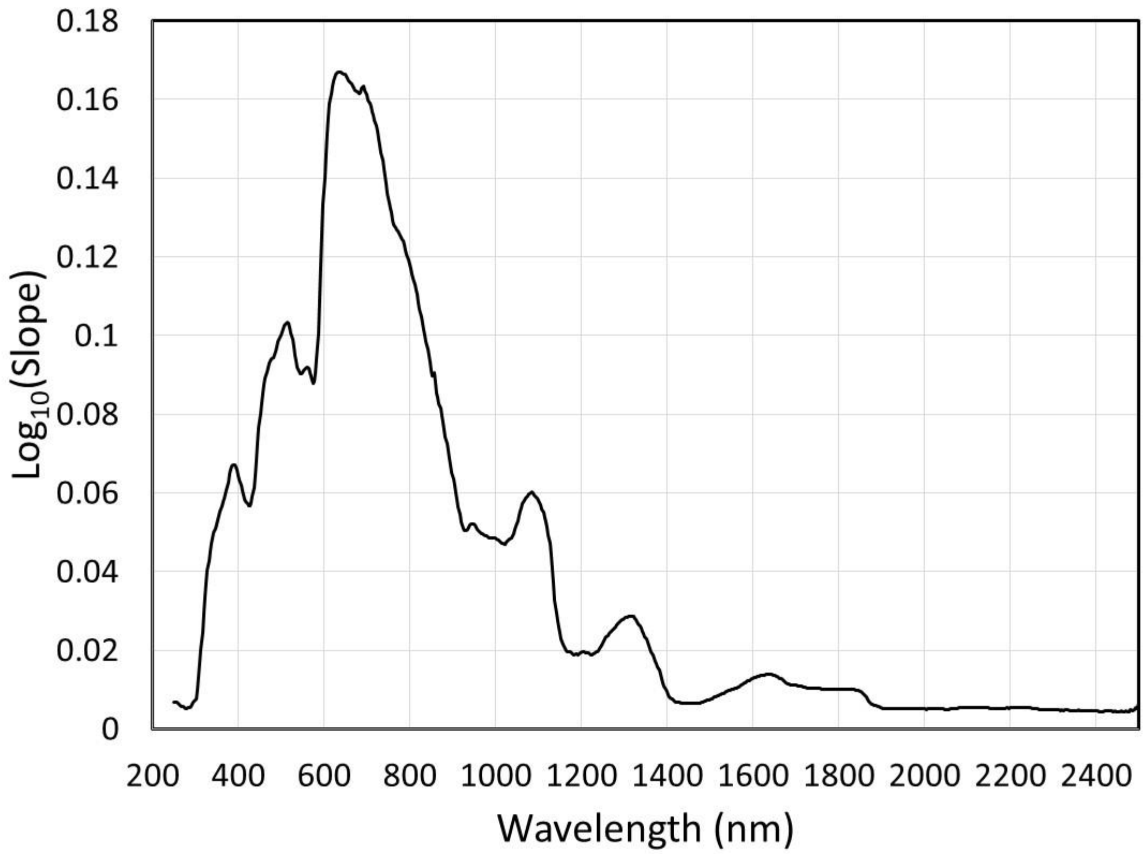

Figure 10. Spectral absorptance of human skin from NIST data.

Variability in scaling and the beam diameter dependence also contribute to the slope, and the standard uncertainties for these sources of variability are listed in Table 7.

Table 7. Sources of variability with values and standard uncertainties, and corresponding standard deviations.

		Standard Deviation	
Source of Variability	Standard Uncertainty (%)	Symbol	Value
MPE Scaling	31	σ_M	0.117
Supra-Threshold Scaling		σ_+	
2nd-Degree Partial	3		0.013
2nd-Degree Full	4		0.017
3rd-Degree	11		0.045
Sub-Threshold Scaling	10	σ_-	0.041

The slope *S* for each source of variability is one plus the standard deviation expressed as a fraction. For example, the slope for MPE Scaling is 1 + 0.31 = 1.31. The standard deviation σ for each source of variability used in the dose-response model is given by Eq. (5) and is also listed in Table 7 with its corresponding symbol. These standard deviations add in quadrature for the final standard deviation. Therefore, for an MVL ED_{50}, the standard deviation is

$$\sigma^2 = \sigma_A^2 + \sigma_M^2 \ , \tag{23}$$

while for a supra-threshold ED_{50}, the standard deviation is

$$\sigma^2 = \sigma_A^2 + \sigma_M^2 + \sigma_+^2 \ , \tag{24}$$

and for a sub-threshold ED_{50}, the standard deviation is

$$\sigma^2 = \sigma_A^2 + \sigma_M^2 + \sigma_-^2 \ . \tag{25}$$

5.0 ANGLE OF INCIDENCE MODEL

The angle of incidence θ_i reduces the effective dose. The effective dose as a function of angle $ED(\theta_i)$ is

$$ED(\theta_\mathrm{i}) = ED(0) \cdot \cos\theta_i \ , \tag{26}$$

resulting in

$$q = \log_{10}\big(ED(\theta_\mathrm{i})\big) = \log_{10}(ED(0)) + \log_{10}(\cos\theta_i) \ . \tag{27}$$

Since the angle of incidence reduces the effective dose, the probability of injury decreases for a fixed effective dose, as illustrated in Fig. 11. Alternatively, the effective dose for a given probability of injury increases with increasing angle of incidence.

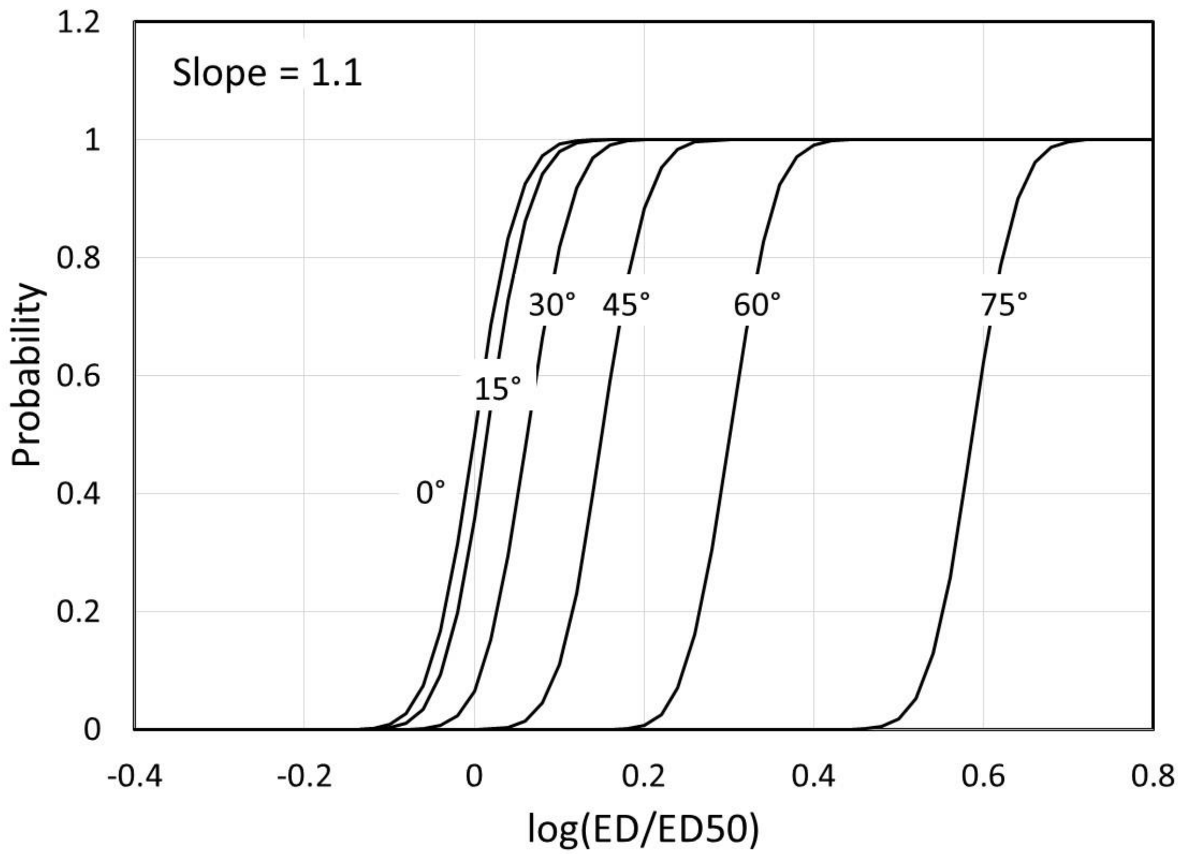

Figure 11. Probability of injury as a function of normalized effective dose for the indicated angles of incidence.

If the angle of incidence is known, Eq. (26) applies. If the angle of incidence is unknown, knowledge of or assumptions about the surface are required. Two tractable surfaces are flat and spherical.

For a flat surface, assuming the incidence direction is uniform over the hemisphere above the surface, the average cosine of the angle of incidence is

$$\langle \cos\theta_{\mathrm{i}} \rangle = \frac{\int_0^{2\pi}\int_0^{\pi/2} \cos\theta\ \sin\theta\ d\theta\ d\phi}{\int_0^{2\pi}\int_0^{\pi/2} \sin\theta\ d\theta\ d\phi} = \frac{1}{2}\,. \tag{28}$$

The average ED is therefore $\frac{1}{2}ED(0)$, so for the average ED to equal the ED_{50}, $ED(0) = 2\ ED_{50}$.

The probability of injury averaged over all incident directions, with $\theta_{\mathrm{i}} = \theta$, is

$$P(q) = \frac{\int_0^{2\pi}\int_0^{\pi/2} \frac{1}{2}\operatorname{erfc}\left[\frac{-(q+\log_{10}(\cos\theta)-\mu)}{\sqrt{2}\sigma}\right] \sin\theta \ d\theta \ d\phi}{\int_0^{2\pi}\int_0^{\pi/2} \sin\theta \ d\theta \ d\phi} \ . \tag{29}$$

Making the substitution $x = \cos\theta$,

$$P(q) = \frac{1}{2}\int_0^1 \operatorname{erfc}\left[\frac{-(q+\log_{10}(x)-\mu)}{\sqrt{2}\sigma}\right] dx \ . \tag{30}$$

A spherical surface is slightly more complicated, and likely more realistic for skin. Assume illumination is uniform over the cross-section of the sphere. The angle of incidence a distance r from the center of a spherical surface with unit radius is

$$cos\theta_i = \sqrt{1-r^2} \, . \tag{31}$$

The average cosine of the angle of incidence is

$$\langle\cos\theta_{\mathrm{i}}\rangle = \frac{\int_0^{2\pi}\int_0^1 \sqrt{1-r^2}\, r\, dr\, d\theta}{\int_0^{2\pi}\int_0^1 r\, dr\, d\theta} = \frac{1/3}{1/2} = \frac{2}{3} \, . \tag{32}$$

In this case, for the average ED to equal the ED_{50}, $ED(0) = \frac{3}{2}ED_{50}$.

The probability of injury averaged over all incident directions is

$$P(q) = \frac{\int_0^{2\pi}\int_0^1 \frac{1}{2}\operatorname{erfc}\left[\frac{-(q+\log_{10}(\cos\theta_{\mathrm{i}})-\mu)}{\sqrt{2}\sigma}\right] r\, dr\, d\theta}{\int_0^{2\pi}\int_0^1 r\, dr\, d\theta} \ . \tag{33}$$

Using Eq. (31) and making the substitution $x = 1 - r^2$,

$$P(q) = \frac{1}{2}\int_0^1 \operatorname{erfc}\left[\frac{-\left(q+\log_{10}\left(x^{1/2}\right)-\mu\right)}{\sqrt{2}\sigma}\right] dx \ . \tag{34}$$

6.0 ED CALCULATION FOR SWEPT SOURCE

The effective dose ED is a spatially averaged radiant exposure with units of J/cm^2, to correspond to the units of MPE for skin. The peak irradiance E_{peak} and exposure duration T typically characterize the exposing laser beam. The average irradiance E_{avg} is given by Eq. (7), with E substituted for H. For a stationary exposure, such as with experiments used to determine an ED_{50}, the exposure duration is the time interval over which the laser was illuminating the skin. An equivalent exposure duration is required if the laser sweeps over the skin. Effects from lasers depend on the energy deposited over a time interval. In general, the radiant exposure H for a time-varying irradiance is

$$H = \int E(t)\, dt \ . \tag{35}$$

If the time dependence of the irradiance is Gaussian, with time interval T_2 between the times when the irradiance is $1/e^2$ of its peak value E_{peak},

$$E(t) = E_{\text{peak}} \cdot \exp\left[-2\left(\frac{2t}{T_2}\right)^2\right] . \tag{36}$$

With this time-dependence of the irradiance, and assigning a maximum exposure duration T_{max}, Eq. (35) becomes

$$H = \int_{-T_{\text{max}}/2}^{T_{\text{max}}/2} E_{\text{peak}} \cdot \exp\left[-2\left(\frac{2t}{T_2}\right)^2\right] dt \ . \tag{37}$$

Now,

$$\int_0^x \exp[-u^2] du = \frac{\sqrt{\pi}}{2} \text{erf}\,(x) \ . \tag{38}$$

Using a change of variables $u = 2\sqrt{2}\frac{t}{T_2}$ and the symmetry of a Gaussian function, Eq. (37) becomes

$$H = 2E_{\text{peak}} \frac{T_2}{2\sqrt{2}} \int_0^{\sqrt{2}T_{\text{max}}/T_2} \exp[-u^2] du = E_{\text{peak}} \frac{\sqrt{\pi}}{2} \frac{T_2}{\sqrt{2}} \text{erf}\left(\sqrt{2}\frac{T_{max}}{T_2}\right) . \tag{39}$$

Therefore, the exposure duration T for which the energy deposited during the exposure is given by $H = E_{\text{avg}} \cdot T$ is

$$T = \frac{\sqrt{\pi}}{2} \frac{T_2}{\sqrt{2}} \text{erf}\left(\sqrt{2}\frac{T_{\text{max}}}{T_2}\right) . \tag{40}$$

If $T_{max} \gg T_2$ then $= \frac{\sqrt{\pi}}{2\sqrt{2}} T_2$, while if $T_{max} \ll T_2$ then $T = T_{max}$.

In all cases, the effective dose is

$$ED = H_{\text{avg}} = E_{\text{avg}} \cdot T\ . \tag{41}$$

7.0 PROBABILITY CALCULATION

Calculating the probability of injury P uses an extension of Eq. (2.2) to account for a variable angle of incidence,

$$P(q) = \frac{1}{2}\int_0^1 erfc\left[\frac{-(q + Log(x^n) - \mu)}{\sqrt{2}\,\sigma}\right]dx\ , \tag{42}$$

where the shape of the surface determines the value of n. For a flat surface, n = 1, while for a spherical surface, n = ½. If the angle of incidence is known, then n = 0 and the effective dose is given by Eq. (26). Probabilities of injury for different surface shapes are shown in Fig. 12.

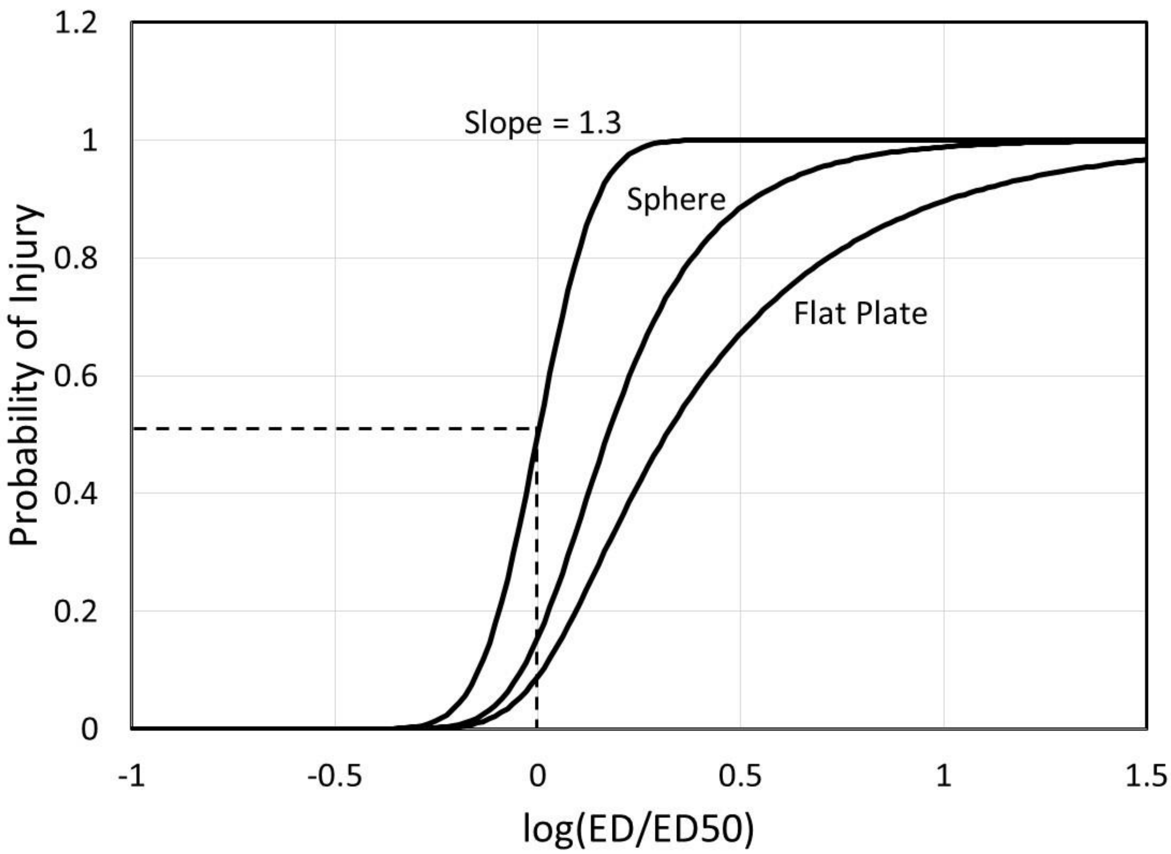

Figure 12. Probability of injury as a function of normalized effective dose for indicated surface shapes.

8.0 EXAMPLE OF INJURY PROBABILITY CALCULATIONS

As an example to illustrate calculating probabilities of injury, consider a laser exposure at a wavelength $\lambda = 1070$ nm. The laser has a peak irradiance $E_{peak} = 500$ W/cm^2, a 1/e^2 beam diameter $D_2 = 5$ cm, and sweeps over the skin with an exposure duration of $T_2 = 500$ ms. This exposure duration is the time interval between irradiances of 1/e^2 of the peak irradiance. What are the probabilities for all injuries, and for different angle of incidence models?

Since the beam is sweeping, the exposure duration T, is given by Eq. (40). While retinal exposures have a $T_{max} = 250$ ms due to saccades and the blink reflex, no such exposure limit applies to the skin so $T_{max} = \infty$ and $T = 313$ ms. The MPE for a wavelength $\lambda = 1070$ nm and exposure duration $T = 313$ ms, from the ANSI Z136.1 standard [7], is MPE = 4.11 J/cm^2, so the MVL ED_{50}, using Eq. (11), is $ED_{50} = 49.4$ J/cm^2. Since the wavelength is 1070 nm, the ED_{50}s for all injuries are calculated using Eqs. (17) to (19), yielding the results given in Table 8.

Table 8. ED_{50} and logarithm for the example for the listed skin injuries.

Injury	ED_{50} (J/cm^2)	μ
Pain	28.6	1.456
MVL (1st-degree)	49.4	1.694
2nd-degree superficial	59.3	1.773
2nd-degree deep	97.3	1.988
3rd-degree	164.8	2.217

From Appendix D, the minimum and maximum human skin absorptance at 1069 nm are 0.3769 and 0.4912, respectively, so using Eq. (22) $\text{slope}_A = \sqrt{0.4912/0.3769} = 1.142$, so $\sigma_A = 0.058$. The standard deviations and slopes for each injury are given in Table 9. Note the standard deviation values are calculated using Eq. (23) to (25), and the slope values are derived from these.

Table 9. Slope and logarithm for the example for the listed skin injuries.

Injury	σ_A	σ_M	σ_-	σ_+	σ	Slope
Pain	0.058	0.117	0.041	-----	0.137	1.371
MVL (1st-degree)	0.058	0.117	-----	-----	0.131	1.352
2nd-degree superficial	0.058	0.117	-----	0.013	0.132	1.355
2nd-degree deep	0.058	0.117	-----	0.017	0.132	1.355
3rd-degree	0.058	0.117	-----	0.045	0.138	1.374

The average irradiance, E_{avg}, by substituting into Eq. (7), is

$$E_{\text{avg}} = \frac{E_{\text{peak}}}{2}\left(\frac{D_2}{0.35\text{ cm}}\right)^2 \left\{1 - \exp\left[-2\left(\frac{0.35\text{ cm}}{D_2}\right)^2\right]\right\} = 497.6\ \text{W/cm}^2\ . \qquad (43)$$

The effective dose, using Eq. (41) and the values for E_{avg} and T is ED = 155.9 J/cm^2, yielding q = 2.193. The probabilities for each injury and angle of incidence model are given in Table 10. As expected, the probability of injury decreases with increasing severity and decreasing average cosine of the angle of incidence.

Table 10. Probabilities for each skin injury type and angle of incidence model for the example.

Angle of Incidence Model			
Injury	Normal	Sphere	Flat
Pain	1.0	0.964	0.812
MVL (1st-degree)	1.0	0.884	0.673
2nd-degree superficial	0.999	0.831	0.607
2nd-degree deep	0.940	0.557	0.360
3rd-degree	0.431	0.147	0.087

Burn injuries are progressive, meaning burns of less severity precede those of a given severity. For example, a person with a 2nd-degree superficial burn injury also experienced a 1st-degree burn during their exposure prior to the more severe burn. The fraction of an exposed population suffering from a burn injury is important, and obtained from the probabilities of injury and their progressive nature. The fraction f of a population with a burn injury indexed by i is

$$f_i = P_i - P_{i+1}\ , \qquad (44)$$

where P is the probability of injury and i+1 is the index of the next-most-severe burn. If there are N severities of burn, and zero indexes no injury, then

$$f_0 = 1 - P_1 \ \text{ and } \ f_N = P_N\ . \qquad (45)$$

Applying Eqs. (44) and (45) to the probabilities in Table 10 results in the population fractions shown in Table 11. Here, zero indexes no pain and N indexes a 3rd-degree burn. Note each column sums to one, and the fractions can vary non-monotonically with burn severity.

Table 11. Fraction of exposed population for each skin injury type and angle of incidence model for the example.

	Angle of Incidence Model		
Injury	Normal	Sphere	Flat
None	0	0.036	0.188
Pain	0	0.080	0.139
MVL (1st-degree)	0.001	0.053	0.066
2nd-degree superficial	0.059	0.274	0.247
2nd-degree deep	0.509	0.410	0.273
3rd-degree	0.431	0.147	0.087

9.0 SUMMARY

A general model for human laser skin dose-response was developed and presented, with the objective of improving the fidelity of models used to assess the risk of skin injury from exposure to laser radiation. The model covers the spectral range from 400 nm to 2000 nm and the temporal range from 1 µs to 10 s. Experimental data and simulation results are the basis of the model, which includes effects from pain to minimal visible lesions to 3rd-degree burns. The model was constructed to capture the essential bio-physical features contributing to human susceptibility to laser injury of the skin, including variability between humans.

The human laser skin dose-response consists of three component models – those for the ED_{50}, the slope, and the angle of incidence. The ED_{50} model includes dependencies on wavelength and exposure duration. It scales the ANSI Z136.1 safety standard MPE to an MVL ED_{50} to achieve both wavelength and exposure duration dependence. All effective doses are the average radiant exposure over the limiting aperture of 3.5 mm diameter. The MVL ED_{50} is further scaled to a supra-threshold ED_{50} for 2nd- and 3rd-degree burns, while the MPE is scaled to a sub-threshold ED_{50} for pain. The slope model includes variability in skin optical absorptance between humans and uncertainties in the ED_{50} model due to scaling and beam diameter dependence. The effective dose depends on the angle of incidence, and the angle of incidence model accounts for two tractable situations. It assumes a uniform probability of direction and calculates an average resulting probability of injury specific to a flat or spherical surface.

While the model for human laser skin dose-response presented here captures the essential bio-physical features, the process of quantifying these features indicated many possible future improvements. Scaling the MPE to an MVL ED_{50} based on sparse experimental data is just one example. Categorizing the bio-physical features as relating to human variability or to scaling helps to organize future improvements. The simple model for human variability, based on skin reflectance, should be significantly expanded by the use of first-principles laser-tissue interaction simulations. With the proper optical and thermal properties of skin tissue layers, the simulation should approximate the human skin reflectance data shown in Fig. 12 and then provide insight on various parts of the body with different tissue layer thicknesses. This high-fidelity simulation would also improve the scaling factors for supra-threshold effects, as would additional experiments evaluating these effects. Carefully chosen and executed experiments could also refine the scaling of MPE to MVL ED_{50}, and the dependence on beam diameter. While there was sufficient experimental data to derive scaling values, additional high-quality experiments would refine and provide more confidence in these values.

10.0 REFERENCES

1. E. Ahmed, E. A. Early, B. J. Lund, and R. J. Thomas, "Human Laser Skin Dose-Response Model," AFRL-RH-FS-TR-2020-0018 (2020).

2. R. Vincelette, G.D. Noojin, C.A. Harbert, K.J. Schuster, A.D. Shingledecker, D. Stolarski, S.S. Kumru, and J.W. Oliver, "Porcine Skin Damage Thresholds for 0.6 to 9.5 cm Beam Diameters from 1070-nm Continuous-Wave Infrared Laser Radiation," J. Biomed. Opt. 19, 035007 (2014)

3. B. Chen, "Experimental and Modeling Study of Thermal Response of Skin and Cornea to Infrared Wavelengths Laser Irradiation," Ph.D. Dissertation, The University of Texas at Austin (2007).

4. J.W. Oliver, R. Vincelette, G.D. Noojin, C.D. Clark, C.A. Harbert, K.J. Schuster, A.D. Shingledecker, S.S. Kumru, J. Maughan, N. Kitzis, G.D. Buffington, D.J. Stolarski, and R.J. Thomas, "Infrared Skin Damage Thresholds from 1319-nm Continuous-Wave Laser Exposures," J. Biomed. Opt. 18, 125002 (2013).

5. J.W. Oliver, D.J. Stolarski, G.D. Noojin, H.M. Hodnett, C.A. Harbert, K.J. Schuster, M.F. Foltz, S.S. Kumru, C.P. Cain, C.J. Finkeldei, G.D. Buffington, I.D. Noojin, and R.J. Thomas, "Infrared Skin Damage Thresholds from 1940-nm Continuous-Wave Laser Exposures," J. Biomed. Opt. 15, 065008 (2010).

6. B. Chen, D.C. O'Dell, S.L. Thomsen, B.A. Rockwell, and A.J. Welsh, "Porcine Skin ED_{50} Damage Thresholds for 2,000 nm Laser Irradiation," Lasers Surg. Med. 37, 373 (2005).

7. American National Standards Institute, "American National Standard for Safe Use of Lasers, ANSI Standard Z136.1-2014," Laser Institute of America (2014).

8. B.G. Zollars, G.J. Elpers, A.L. Goodwin, E.A. Early, N.J. Gamez, and R.J. Thomas, "Scalable Effects Simulation Environment (SESE) Version 2.5.0," AFRL-RH-FS-TR-2019-0016 (2019).

9. M.P. DeLisi, M.S. Schmidt, A.F. Hoffman, A.M. Peterson, G.D. Noojin, A.D. Shingledecker, A.R. Boretsky, D.J. Stolarski, S.S. Kumru, and R.J. Thomas, "Thermal Damage Thresholds for Multipe-Pulse Porcine Skin Laser Exposures at 1070 nm," J. Biomed. Opt. 25, 035001 (2019).

10. E. Ahmed, E. Early, P. Kennedy, and R. Thomas, "Human Laser Retinal Dose-Response Model," AFRL-RH-FS-TR-2018-0006 (2018).

11. R.J. Rockwell, Jr. and L. Goldman, "Research on Human Skin Laser Damage Thresholds," United States Air Force Aerospace Medical Division, DERM-LL-74-1003 (1974).

12. Li Zhoazhang, “Laser Safety, Protection Standards Reviewed,” Yingyong Jiguang 3, 141 (1986).

13. E. M. Renz and L. C. Cancio, “Acute Burn Care” in E. Savitsky and B. Eastridge, *Combat Casualty Care, Lessons Learned from OEF and OIF,* Borden Institute, Fort Detrick, Maryland (2012).

14. M. L. Denton, E. M. Ahmed, G. D. Noojin, A. J. Tijerina, G. Gamboa, C. C. Gonzalez, and B. A. Rockwell, “Effect of Ambient Temperature and Intracellular Pigmentation on Photothermal Damage Rate Kinetics,” J. Biomed. Opt. 24, 065002 (2019).

15. E. M. Ahmed, G. D. Noojin, and M. L. Denton, “Damage Integral and Other Predictive Formulas for Nonisothermal Heating during Laser Exposure,” J. Biomed. Opt. 27, 035001 (2022).

16. C.-y. Lyu and R.-j. Zhan, “Accurate Analysis of Limiting Human Dose of Non-Lethal Laser Weapons,” Defence Technology 18, 678-688 (2022).

17. A. M. Stoll and L. C. Green, “The Relationship Between Pain and Tissue Damage Due to Thermal Radiation,” NADC-MA-5808 (1958).

18. A. M. Stoll and M. A. Chianti, “A Method and Rating System for Evaluation of Thermal Protection,” NADC-MR-6809 (1968).

19. L. Arendt-Nielsen and P. Bjerring, “Sensory and Pain Threshold Characteristics to Laser Stimuli,” J. Neurology, Neurosurgery, and Psychiatry 51, 35-42 (1988).

20. D. Tata, V. I. Villavicencio, M. C. Cook, T. E. Dayton, C. D. Clark, C. A. Moreno, J. A. Ross, J. S. Eggers, P. Kennedy, D. Christensen, and J. Notabartolo, “Infra Red Laser Induced Skin Damage and Perception,” AFRL-HE-BR-TR-2005-0139 (2005).

21. M. P. DeLisi, A. M. Peterson, L. A. Lile, G. D. Noojin, A. D. Shingledecker, D. J. Stolarski, C. A. Oian, S. S. Kumru, and R. J. Thomas, “Suprathreshold Laser Injuries in Excised Porcine Skin for Millisecond Exposures at 1070 nm,” J. Biomed. Opt. 23, 125001 (2018).

22. T. B. Fitzpatrick, “Sun and Skin,” Journal de Medecine Esthetique 2, 33 (1975).

23. S. L. Jacques, “Optical Properties of Biological Tissues: A Review,” Phys. Med. Biol. 58, R37 (2013).

24. C. C. Cooksey, D.W. Allen, and B.K. Tsai, “Reference Data Set of Human Skin Reflectance,” J. Res. Natl. Inst. Stan. Tech. 122, 26 (2017).

APPENDIX A. ED_{50} Experimental Data

Research papers with ED_{50} results for skin exposures report those values using a variety of quantities. The references cited in Section 3 use energy, power, or radiant exposure for ED_{50}. In addition, the calculations of radiant exposure are not consistent. The following tables present the data reported in the references and the process to calculate all values of ED_{50} as radiant exposure averaged over a limiting aperture with a diameter of 3.5 mm.

All the experimental data in this Appendix was obtained using Yorkshire mini-pigs and single pulses, and all report exposure durations and $1/e^2$ beam diameters. The sections are arranged by increasing wavelength, with relevant experimental parameters and calculations detailed. The average and standard deviation of the ratio of average radiant exposure to MPE are also included for each set of experimental data.

A.1 1070 nm

A.1.1 Primary

Reference: Vincelette [2]

Calculation of H_{avg}: ED_{50} reported in energy Q, so calculation of H_{peak} and H_{avg} uses Eqs. (6) and (7)

Table A.1. Experimental data, calculated average radiant exposure, and ratio to MPE for Ref. [2]

D_2 (cm)	T (s)	Q_{50} (J)		H_{peak} (J/cm^2)	H_{avg} (J/cm^2)		MPE (J/cm^2)	H_{avg}/MPE
0.6	0.01	4.0		28.3	20.5		1.74	11.80
0.6	0.07	11.1		78.5	57.0		2.83	20.13
0.6	10	57.1		403.9	293.0		9.78	29.96
1.1	0.01	16.1		33.9	30.7		1.74	17.64
1.1	0.1	22.6		47.6	43.1		3.09	13.92
1.1	10	82		172.6	156.2		9.78	15.97
1.9	0.05	48.6		34.3	33.1		2.60	12.74
1.9	0.25	74.2		52.3	50.6		3.89	13.01
1.9	10	154		108.6	105.0		9.78	10.74
2.4	0.01	46.6		20.6	20.2		1.74	11.60
2.4	0.025	43		19.0	18.6		2.19	8.51
2.4	0.25	55.3		24.4	23.9		3.89	6.15
4.7	0.025	213.3		24.6	24.5		2.19	11.18
4.7	0.1	267		30.8	30.6		3.09	9.90
4.7	0.25	295		34.0	33.8		3.89	8.70
9.5	0.25	1125		31.7	31.7		3.89	8.15
							Average	12.0
							Standard Deviation	3.76

Note: the average of H_{avg}/MPE does not include the ratio for D_2 = 0.6 cm and T = 10 s due to its anomalously large value.

A.1.2 Secondary

Reference: DeLisi [3]

Calculation of H_{avg}: ED_{50} reported in radiant exposure H, stated as the energy divided by the $1/e^2$ beam area. The peak radiant exposure is twice this value, and calculation of H_{avg} uses Eq. (7).

Table A.2. Experimental data, calculated average radiant exposure, and ratio to MPE for Ref. [3]

D_2 (cm)	T (s)	H_{50} (J/cm^2)		H_{peak} (J/cm^2)	H_{avg} (J/cm^2)		MPE (J/cm^2)	H_{avg}/MPE
1.04	0.01	17.8		35.6	31.9		1.74	18.3
1.04	0.1	33.2		66.4	59.4		3.09	19.2
0.973	10	83.7		167.4	147.5		9.78	15.1
							Average	17.5
							Standard Deviation	2.17

A.2 1214 nm

Reference: Chen [4]

Calculation of H_{avg}: ED_{50} reported in power Φ, so convert power to energy using Eq. (10), then calculate H_{peak} and H_{avg} using Eqs. (6) and (7)

Table A.3. Experimental data, calculated average radiant exposure, and ratio to MPE for Ref. [4]

D_2 (cm)	T (s)	Φ_{50} (J)		H_{peak} (J/cm^2)	H_{avg} (J/cm^2)		MPE (J/cm^2)	H_{avg}/MPE
0.6	0.981	8.6		59.7	43.3		5.47	7.9
0.6	3.05	3.66		79.0	57.3		7.27	7.9
0.6	9.81	1.3		90.2	65.4		9.73	6.7
0.8	0.981	14.1		55.0	45.7		5.47	8.4
0.8	9.81	1.76		68.7	57.1		9.73	5.9
1	0.981	23		57.5	51.0		5.47	9.3
1	3.05	7		54.4	48.2		7.27	6.6
1	9.81	2.67		66.7	59.2		9.73	6.1
							Average	7.34
							Standard Deviation	1.21

A.3 1319 nm

Reference: Oliver [5]

Calculation of H_{avg}: ED_{50} reported in energy Q, so calculation of H_{peak} and H_{avg} uses Eqs. (6) and (7)

Table A.4. Experimental data, calculated average radiant exposure, and ratio to MPE for Ref. [5]

D_2 (cm)	T (s)	Q_{50} (J)		H_{peak} (J/cm^2)	H_{avg} (J/cm^2)		MPE (J/cm^2)	H_{avg}/MPE
0.61	0.25	6.25		42.8	31.3		3.9	8.7
0.61	1	6.22		42.6	31.2		5.5	8.7
0.61	2.5	7.38		50.5	37.0		6.9	9.1
0.61	10	9.11		62.3	45.7		9.8	9.6
0.97	0.25	13.38		36.2	31.9		3.9	10.5
0.97	1	13.7		37.1	32.6		5.5	10.6
0.97	2.5	15.1		40.9	36.0		6.9	10.8
0.97	10	18.7		50.6	44.6		9.8	11.4
							Average	9.92
							Standard Deviation	1.06

A.4 1940 nm

Reference: Oliver [6]

Calculation of H_{avg}: ED_{50} reported in energy Q, so calculation of H_{peak} and H_{avg} uses Eqs. (6) and (7)

Table A.5. Experimental data, calculated average radiant exposure, and ratio to MPE for Ref. [6]

D_2 (cm)	T (s)	Q_{50} (J)		H_{peak} (J/cm^2)	H_{avg} (J/cm^2)		MPE (J/cm^2)	H_{avg}/MPE
0.48	0.01	0.201		2.2	1.4		0.2	7.7
0.48	0.07	0.817		9.0	5.6		0.3	19.3
0.48	10	2.02		22.3	13.7		1.0	13.8
1	0.05	1.16		3.0	2.6		0.3	9.9
1.8	0.07	3.73		2.9	2.8		0.3	9.8
1.8	10	5.72		4.5	4.3		1.0	4.3
							Average	10.8
							Standard Deviation	5.18

A.5 2000 nm

Reference: Chen [7]

Calculation of H_{avg}: ED_{50} reported in energy Q, so calculation of H_{peak} and H_{avg} uses Eqs. (6) and (7)

Table A.6. Experimental data, calculated average radiant exposure, and ratio to MPE for Ref. [7]

D_2 (cm)	T (s)	Q_{50} (J)		H_{peak} (J/cm^2)	H_{avg} (J/cm^2)		MPE (J/cm^2)	H_{avg}/MPE
0.483	0.25	2.62		7.1	4.4		0.40	11.2
0.483	0.5	1.49		8.1	5.0		0.47	10.7
0.483	1	0.93		10.2	6.3		0.56	11.2
0.483	2.5	0.41		11.2	6.9		0.70	9.8
0.965	0.25	8.46		5.8	5.1		0.40	12.8
0.965	0.5	4.94		6.8	5.9		0.47	12.6
0.965	1	2.88		7.9	6.9		0.56	12.4
0.965	2.5	1.41		9.6	8.5		0.70	12.0
1.465	0.25	16.09		4.8	4.5		0.40	11.4
1.465	0.5	8.46		5.0	4.7		0.47	10.1
1.465	1	5.02		6.0	5.6		0.56	10.1
1.465	2.5	2.46		7.3	6.9		0.70	9.8
							Average	11.2
							Standard Deviation	1.11

APPENDIX B. Simulation Data

Table B.1. Threshold powers for burn degrees determined from simulations and ratios to 1st-degree burn powers

		Burn Degree				Ratio to 1st-Degree Burn		
		1st	2nd Superficial	2nd Deep	3rd	2nd Super.	2nd Deep	3rd
D_2 (cm)	T (s)	Power (W)						
1	0.1	606.62	779.36	1600.6	3748.2	1.28	2.64	6.18
3	0.1	4753.9	5964.2	11520	21031	1.25	2.42	4.42
10	0.1	52440	65634	128290	230920	1.25	2.45	4.40
30	0.1	482330	617660	1126200	2412200	1.28	2.33	5.00
1	0.3	241.99	287.79	506.61	1034.2	1.19	2.09	4.27
3	0.3	1890.1	2235	3667.5	6222.7	1.18	1.94	3.29
10	0.3	20729	24476	40136	54627	1.18	1.94	2.64
30	0.3	191210	227120	359960	582460	1.19	1.88	3.05
1	0.5	174.977	183.27	299.774	503.021	1.05	1.71	2.87
1.5	0.5	297.48	386.213	592.507	1013.13	1.30	1.99	3.41
2	0.5	523.258	660.88	1003.472	1506.421	1.26	1.92	2.88
2.5	0.5	828.952	1041.024	1535.92	2260.417	1.26	1.85	2.73
3	0.5	1151.729	1425.872	2162.235	3454.042	1.24	1.88	3.00
5	0.5	3113.1	3913.755	5613.104	8748.437	1.26	1.80	2.81
10	0.5	14898.71	15573.52	23406.61	32431.37	1.05	1.57	2.18
15	0.5	27580	35274.08	51303.07	86166.06	1.28	1.86	3.12
20	0.5	52359.94	60641.37	89343.75	131275.2	1.16	1.71	2.51
1	1	87.146	99.961	150.27	239.6	1.15	1.72	2.75
3	1	676.04	772.71	1047.9	1467.9	1.14	1.55	2.17
10	1	7356.3	8402.8	11367	15802	1.14	1.55	2.15
30	1	67222	76832	102000	129300	1.14	1.52	1.92
1	1	87.198	99.802	145.389	234.711	1.14	1.67	2.69
1.5	1	182.123	208.24	289.281	439.272	1.14	1.59	2.41
2	1	311.685	357.161	487.285	703.78	1.15	1.56	2.26
2.5	1	486.931	557.053	743.777	1079.037	1.14	1.53	2.22

		Burn Degree				Ratio to 1st-Degree Burn		
		1st	2nd Superficial	2nd Deep	3rd	2nd Super.	2nd Deep	3rd
D_2 (cm)	T (s)	Power (W)						
3	1	675.941	771.664	1037.747	1368.145	1.14	1.54	2.02
5	1	1790.931	2101.169	2723.774	4004.945	1.17	1.52	2.24
10	1	7163.423	8458.545	11287.51	15111.62	1.18	1.58	2.11
15	1	16618.05	18968.11	24724.67	32635.26	1.14	1.49	1.96
20	1	28403.43	32460.43	43350.24	62498.18	1.14	1.53	2.20
1	1.5	61.606	70.694	94.519	137.755	1.15	1.53	2.24
1.5	1.5	128.025	145.684	189.469	253.386	1.14	1.48	1.98
2	1.5	215.092	246.613	318.458	440.108	1.15	1.48	2.05
2.5	1.5	336.792	386.96	483.383	616.866	1.15	1.44	1.83
3	1.5	474.318	544.863	689.352	896.886	1.15	1.45	1.89
5	1.5	1283.493	1463.929	1779.078	2293.102	1.14	1.39	1.79
10	1.5	5137.36	5824.645	7451.543	9438.393	1.13	1.45	1.84
15	1.5	11589.19	13258.82	16372.72	21801.02	1.14	1.41	1.88
20	1.5	19795.29	22565.49	27992.56	37788.72	1.14	1.41	1.91
1	2	48.265	54.999	70.824	101.386	1.14	1.47	2.10
1.5	2	99.754	114.135	141.232	187.64	1.14	1.42	1.88
2	2	170.194	194.245	236.484	305.804	1.14	1.39	1.80
2.5	2	262.793	299.086	359.195	443.522	1.14	1.37	1.69
3	2	368.327	413.474	505.629	772.702	1.12	1.37	2.10
5	2	992.606	1135.71	1345.276	1549.74	1.14	1.36	1.56
10	2	3768.055	4504.596	5529.038	7029.161	1.20	1.47	1.87
15	2	8962.075	10074.09	12151.85	21114.25	1.12	1.36	2.36
20	2	15265.7	17250.91	20914.66	25567.87	1.13	1.37	1.67
1	2.5	40.079	45.659	56.618	77.604	1.14	1.41	1.94
1.5	2.5	81.312	93.664	111.523	142.682	1.15	1.37	1.75
2	2.5	140.111	159.61	187.793	224.881	1.14	1.34	1.61
2.5	2.5	216.047	241.568	283.97	332.53	1.12	1.31	1.54
3	2.5	303.039	341.378	400.51	441.938	1.13	1.32	1.46
5	2.5	815.609	923.385	1064.886	1290.666	1.13	1.31	1.58

		Burn Degree				Ratio to 1st-Degree Burn		
		1st	2nd Superficial	2nd Deep	3rd	2nd Super.	2nd Deep	3rd
D_2 (cm)	T (s)	Power (W)						
10	2.5	3233.963	3747.89	4339.396	5181.5	1.16	1.34	1.60
15	2.5	7267.941	8320.596	9614.889	11562.73	1.14	1.32	1.59
20	2.5	12578.63	13801.6	16641.06	20336.99	1.10	1.32	1.62
1	3	34.494	39.306	47.475	63.315	1.14	1.38	1.84
1.5	3	70.368	80.063	93.462	108.732	1.14	1.33	1.55
2	3	119.553	134.944	156.029	178.171	1.13	1.31	1.49
2.5	3	184.02	207.12	237.016	271.054	1.13	1.29	1.47
3	3	258.339	285.792	333.751	383.248	1.11	1.29	1.48
5	3	694.318	793.868	874.434	1021.067	1.14	1.26	1.47
10	3	2772.498	3181.164	3555.326	4106.306	1.15	1.28	1.48
15	3	6245.857	7062.569	7906.343	8775.812	1.13	1.27	1.41
20	3	10704.22	11733.06	13690.89	15980.08	1.10	1.28	1.49

APPENIX C. Sub-Threshold Data

C.1 Broadband

References: Stoll [17] and Stoll [18]

Calculation of *H*: Convert irradiance *E* in cal/(cm^2 s) to J/cm^2 using 1 cal = 4.184 J, then calculate *H* using Eq. (9)

Table C.1. Radiant exposure thresholds for pain and blister (2nd-superficial) burn for Refs. [17] and [18]

	Pain Threshold		Blister Threshold		
Irradiance (cal/(cm^2 s))	*T* (s)	*H* (J/cm^2)	*T* (s)	*H* (J/cm^2)	Ref.
0.1	13.5	5.65	33.8	14.1	14
0.125	10.2	5.28	---	---	14
0.15	7.8	4.90	20.8	13.1	14
0.2	5.5	4.60	13.4	11.2	14
0.3	2.9	3.64	7.8	9.79	14
0.4	2.2	3.68	5.6	9.37	14
0.6	---	---	3.0	7.53	15
0.8	---	---	1.95	6.53	15
1.0	---	---	1.41	5.90	15
1.2	---	---	1.08	5.42	15

C.2 2000 nm

Reference: Tata [20]

Calculation of H_{avg}: ED_{50} reported in radiant exposure H, stated as the energy divided by the $1/e^2$ beam area. The peak radiant exposure is twice this value, and H_{avg} is calculated using Eq. (7).

Table C.2. Experimental data, calculated average radiant exposure, and ratio to MPE for ED_{50} for Ref. [20]

D_2 (cm)	T (s)	H_{50} (J/cm^2)		H_{peak} (J/cm^2)	H_{avg} (J/cm^2)		MPE (J/cm^2)	H_{avg}/MPE
0.5	0.25	2.46		4.92	3.14		0.40	7.85
0.5	0.50	5.46		10.92	6.96		0.47	14.8
0.5	1.0	5.08		10.16	6.48		0.56	11.6
0.5	2.5	5.50		11.0	7.01		0.70	10.0
1.5	0.25	2.39		4.78	4.53		0.40	11.3
1.5	0.50	2.51		5.02	4.76		0.47	10.1
1.5	1.0	2.98		5.96	5.65		0.56	10.1
1.5	2.5	3.65		7.30	6.92		0.70	9.9

Table C.3. Experimental data, calculated average radiant exposure, and ratio to MPE for sensation on the hand for Ref. [20]

D_2 (cm)	T (s)	H_{50} (J/cm^2)		H_{peak} (J/cm^2)	H_{avg} (J/cm^2)		MPE (J/cm^2)	H_{avg}/MPE
1.5	0.25	0.542		1.084	1.027		0.40	2.56
1.5	2.5	1.02		2.04	1.93		0.70	2.76

Table C.4. Experimental data, calculated average radiant exposure, and ratio to MPE for sensation on the forehead for Ref. [20]

D_2 (cm)	T (s)	H_{50} (J/cm^2)		H_{peak} (J/cm^2)	H_{avg} (J/cm^2)		MPE (J/cm^2)	H_{avg}/MPE
1.5	0.25	0.068		0.136	0.129		0.40	0.32
1.5	2.5	0.30		0.60	0.57		0.70	0.81

C.3 1070 nm

Reference: DeLisi [21]

Calculation of H_{avg}: ED_{50} reported in radiant exposure H, stated as the energy divided by the $1/e^2$ beam area. The peak radiant exposure is twice this value, and H_{avg} is calculated using Eq. (7).

Table C.5. Experimental data, calculated average radiant exposure, and ratio for MVL and bubble effects for Ref. [21]

		MVL		Bubble		
D_2 (cm)	T (ms)	H_{50} (J/cm^2)	H_{avg} (J/cm^2)	H_{50} (J/cm^2)	H_{avg} (J/cm^2)	Bubble/MVL
3	3	28.3	19.4	35.1	24.1	1.24
7	100	95.5	150.1	141	221.9	1.48

APPENDIX D. Human Skin Spectral Absorptance Range

Table D.1. Minimum and maximum spectral absorptance of human skin

	Absorptance				Absorptance	
Wavelength (nm)	Minimum	Maximum		Wavelength (nm)	Minimum	Maximum
250	0.9263	0.9563		379	0.7053	0.9508
253	0.9269	0.9569		382	0.7011	0.9502
256	0.9281	0.9574		385	0.6984	0.9496
259	0.9295	0.9581		388	0.6967	0.9488
262	0.9312	0.9587		391	0.6963	0.9480
265	0.9328	0.9593		394	0.6971	0.9474
268	0.9341	0.9593		397	0.6993	0.9466
271	0.9351	0.9597		400	0.7028	0.9459
274	0.9357	0.9598		403	0.7066	0.9452
277	0.9367	0.9599		406	0.7102	0.9446
280	0.937	0.9600		409	0.7137	0.9437
283	0.9368	0.9602		412	0.7171	0.9430
286	0.9365	0.9603		415	0.7197	0.9422
289	0.9351	0.9604		418	0.7217	0.9415
292	0.9331	0.9605		421	0.723	0.9408
295	0.9314	0.9606		424	0.7238	0.9400
298	0.9299	0.9609		427	0.7229	0.9391
301	0.9275	0.9611		430	0.7194	0.9381
304	0.9169	0.9611		433	0.7136	0.9370
307	0.9039	0.9610		436	0.7051	0.9358
310	0.8905	0.9609		439	0.6939	0.9343
313	0.875	0.9607		442	0.68	0.9326
316	0.8574	0.9605		445	0.6656	0.9307
319	0.8388	0.9601		448	0.652	0.9286
322	0.8224	0.9594		451	0.6407	0.9266
325	0.8083	0.9586		454	0.6312	0.9248
328	0.7958	0.9579		457	0.6229	0.9228
331	0.7856	0.9573		460	0.6155	0.9212
334	0.777	0.9568		463	0.6094	0.9195
337	0.7699	0.9564		466	0.6043	0.9178
340	0.7645	0.9562		469	0.5999	0.9164
343	0.7596	0.9559		472	0.5965	0.9150
346	0.7555	0.9556		475	0.5939	0.9135
349	0.7515	0.9552		478	0.5913	0.9122
352	0.7475	0.9550		481	0.5895	0.9110
355	0.7434	0.9546		484	0.5866	0.9097
358	0.7393	0.9541		487	0.5833	0.9082
361	0.7348	0.9538		490	0.5795	0.9067
364	0.7309	0.9534		493	0.5752	0.9053
367	0.727	0.9528		496	0.5716	0.9036
370	0.7232	0.9522		499	0.569	0.9021
373	0.7192	0.9516		502	0.5657	0.9006
376	0.7128	0.9515		505	0.5626	0.8992

Table D.1 (cont.) Minimum and maximum spectral absorptance of human skin

	Absorptance				Absorptance	
Wavelength (nm)	Minimum	Maximum		Wavelength (nm)	Minimum	Maximum
508	0.56	0.8978		652	0.3417	0.7336
511	0.5578	0.8965		655	0.3405	0.7292
514	0.5565	0.8954		658	0.3394	0.7249
517	0.5566	0.8944		661	0.338	0.7204
520	0.5582	0.8935		664	0.3365	0.7158
523	0.5614	0.8929		667	0.3352	0.7112
526	0.5657	0.8926		670	0.3337	0.7065
529	0.5707	0.8923		673	0.3323	0.7020
532	0.5757	0.8918		676	0.3306	0.6973
535	0.5796	0.8913		679	0.329	0.6926
538	0.5829	0.8907		682	0.327	0.6879
541	0.5855	0.8900		685	0.3244	0.6834
544	0.5865	0.8891		688	0.3205	0.6786
547	0.5859	0.8879		691	0.3174	0.6735
550	0.5838	0.8864		694	0.3168	0.6687
553	0.5813	0.8847		697	0.3152	0.6643
556	0.5789	0.8830		700	0.3144	0.6602
559	0.5769	0.8811		703	0.314	0.6558
562	0.5759	0.8791		706	0.3133	0.6520
565	0.5756	0.8774		709	0.3128	0.6483
568	0.5771	0.8758		712	0.3125	0.6439
571	0.5812	0.8746		715	0.3121	0.6399
574	0.5827	0.8732		718	0.312	0.6358
577	0.5798	0.8712		721	0.3119	0.6322
580	0.5724	0.8681		724	0.3121	0.6285
583	0.5599	0.8636		727	0.3132	0.6248
586	0.5397	0.8577		730	0.3139	0.6217
589	0.515	0.8507		733	0.3151	0.6186
592	0.4908	0.8431		736	0.3167	0.6160
595	0.468	0.8354		739	0.318	0.6127
598	0.4476	0.8276		742	0.3193	0.6097
601	0.4297	0.8200		745	0.3204	0.6065
604	0.4142	0.8126		748	0.3226	0.6038
607	0.4015	0.8058		751	0.3246	0.6010
610	0.3909	0.7996		754	0.3254	0.5984
613	0.3818	0.7939		757	0.3256	0.5956
616	0.3747	0.7885		760	0.3265	0.5924
619	0.3691	0.7833		763	0.3263	0.5890
622	0.3646	0.7782		766	0.3253	0.5850
625	0.3608	0.7735		769	0.3238	0.5808
628	0.3573	0.7691		772	0.3218	0.5763
631	0.3543	0.7646		775	0.3199	0.5717
634	0.3521	0.7600		778	0.3188	0.5680
637	0.3501	0.7556		781	0.318	0.5642
640	0.348	0.7512		784	0.317	0.5611
643	0.3464	0.7468		787	0.3166	0.5580
646	0.3449	0.7425		790	0.3166	0.5547
649	0.3432	0.7381		793	0.3167	0.5515

Table D.1 (cont.) Minimum and maximum spectral absorptance of human skin

	Absorptance				Absorptance	
Wavelength (nm)	Minimum	Maximum		Wavelength (nm)	Minimum	Maximum
796	0.3167	0.5484		940	0.4187	0.5318
799	0.3164	0.5450		943	0.4221	0.5363
802	0.3163	0.5420		946	0.4256	0.5411
805	0.3169	0.5396		949	0.4297	0.5464
808	0.3167	0.5370		952	0.4344	0.5515
811	0.3178	0.5349		955	0.4392	0.5564
814	0.3185	0.5326		958	0.4436	0.5603
817	0.3189	0.5304		961	0.4466	0.5626
820	0.3205	0.5280		964	0.4481	0.5636
823	0.3217	0.5260		967	0.4489	0.5643
826	0.3237	0.5245		970	0.4495	0.5650
829	0.3256	0.5235		973	0.4502	0.5654
832	0.3275	0.5226		976	0.4507	0.5653
835	0.3287	0.5212		979	0.4506	0.5646
838	0.3298	0.5193		982	0.4501	0.5635
841	0.3313	0.5171		985	0.4492	0.5620
844	0.3327	0.5153		988	0.4479	0.5604
847	0.3334	0.5126		991	0.4465	0.5586
850	0.3355	0.5105		994	0.4449	0.5564
853	0.3366	0.5087		997	0.4431	0.5540
856	0.3350	0.5081		1000	0.4412	0.5517
859	0.3385	0.5081		1003	0.4396	0.5492
862	0.3423	0.5075		1006	0.4377	0.5463
865	0.3435	0.5062		1009	0.4357	0.5431
868	0.3451	0.5052		1012	0.4337	0.5399
871	0.3467	0.5045		1015	0.4317	0.5367
874	0.3490	0.5038		1018	0.4296	0.5336
877	0.3514	0.5033		1021	0.4271	0.5304
880	0.3540	0.5028		1024	0.4239	0.5272
883	0.3569	0.5025		1027	0.4207	0.5241
886	0.3599	0.5027		1030	0.4177	0.5210
889	0.3633	0.5027		1033	0.4148	0.5181
892	0.3664	0.5028		1036	0.4118	0.5152
895	0.3693	0.5030		1039	0.4085	0.5121
898	0.3726	0.5033		1042	0.4049	0.5092
901	0.3760	0.5040		1045	0.4011	0.5065
904	0.3795	0.5046		1048	0.3974	0.5039
907	0.3832	0.5054		1051	0.3934	0.5018
910	0.3873	0.5066		1054	0.3894	0.4997
913	0.3916	0.5080		1057	0.3857	0.4977
916	0.3963	0.5093		1060	0.3824	0.4955
919	0.4008	0.5110		1063	0.3793	0.4939
922	0.4046	0.5134		1066	0.3769	0.4926
925	0.4080	0.5158		1069	0.3749	0.4912
928	0.4110	0.5183		1072	0.3736	0.4903
931	0.4131	0.5210		1075	0.3725	0.4895
934	0.4148	0.5240		1078	0.3716	0.4893
937	0.4165	0.5276		1081	0.3710	0.4894

Table D.1 (cont.) Minimum and maximum spectral absorptance of human skin

	Absorptance				Absorptance	
Wavelength (nm)	Minimum	Maximum		Wavelength (nm)	Minimum	Maximum
1084	0.3709	0.4893		1228	0.6450	0.7046
1087	0.3716	0.4897		1231	0.6376	0.6974
1090	0.3727	0.4903		1234	0.6312	0.6908
1093	0.3741	0.4913		1237	0.6255	0.6850
1096	0.3759	0.4927		1240	0.6206	0.6799
1099	0.3778	0.4940		1243	0.6144	0.6749
1102	0.3803	0.4959		1246	0.6085	0.6708
1105	0.3830	0.4979		1249	0.6034	0.6670
1108	0.3862	0.4995		1252	0.5988	0.6637
1111	0.3894	0.5017		1255	0.5949	0.6610
1114	0.3934	0.5040		1258	0.5917	0.6591
1117	0.3980	0.5071		1261	0.5892	0.6575
1120	0.4036	0.5110		1264	0.5869	0.6563
1123	0.4114	0.5167		1267	0.5854	0.6555
1126	0.4216	0.5240		1270	0.5844	0.6554
1129	0.4351	0.5336		1273	0.5840	0.6558
1132	0.4528	0.5463		1276	0.5838	0.6569
1135	0.4740	0.5620		1279	0.5840	0.6584
1138	0.4980	0.5791		1282	0.5848	0.6603
1141	0.5230	0.5987		1285	0.5860	0.6628
1144	0.5476	0.6216		1288	0.5877	0.6658
1147	0.5695	0.6416		1291	0.5897	0.6694
1150	0.5888	0.6589		1294	0.5926	0.6735
1153	0.6052	0.6725		1297	0.5961	0.6779
1156	0.6189	0.6834		1300	0.6002	0.6834
1159	0.6284	0.6919		1303	0.6051	0.6898
1162	0.6360	0.6986		1306	0.6106	0.6962
1165	0.6416	0.7035		1309	0.6165	0.7035
1168	0.6453	0.7068		1312	0.6232	0.7113
1171	0.6478	0.7091		1315	0.6303	0.7196
1174	0.6503	0.7117		1318	0.6382	0.7283
1177	0.6534	0.7145		1321	0.6467	0.7375
1180	0.6571	0.7179		1324	0.6558	0.7468
1183	0.6617	0.7220		1327	0.6655	0.7562
1186	0.6652	0.7260		1330	0.6752	0.7655
1189	0.6683	0.7295		1333	0.6848	0.7743
1192	0.6710	0.7322		1336	0.6943	0.7828
1195	0.6724	0.7343		1339	0.7034	0.7911
1198	0.6736	0.7360		1342	0.7122	0.7988
1201	0.6746	0.7380		1345	0.7207	0.8059
1204	0.6755	0.7392		1348	0.7287	0.8121
1207	0.6759	0.7398		1351	0.7367	0.8182
1210	0.6758	0.7393		1354	0.7446	0.8239
1213	0.6742	0.7369		1357	0.7525	0.8296
1216	0.6708	0.7330		1360	0.7605	0.8353
1219	0.6664	0.7273		1363	0.7686	0.8416
1222	0.6604	0.7200		1366	0.7774	0.8481
1225	0.6529	0.7123		1369	0.7870	0.8554

Table D.1 (cont.) Minimum and maximum spectral absorptance of human skin

	Absorptance				Absorptance	
Wavelength (nm)	Minimum	Maximum		Wavelength (nm)	Minimum	Maximum
1372	0.7974	0.8636		1516	0.9039	0.9393
1375	0.8080	0.8723		1519	0.9024	0.9384
1378	0.8194	0.8815		1522	0.9009	0.9375
1381	0.8321	0.8918		1525	0.8994	0.9365
1384	0.8460	0.9021		1528	0.8978	0.9354
1387	0.8592	0.9115		1531	0.8961	0.9344
1390	0.8708	0.9194		1534	0.8944	0.9333
1393	0.8804	0.9262		1537	0.8926	0.9322
1396	0.8889	0.9317		1540	0.8908	0.9310
1399	0.8960	0.9360		1543	0.8891	0.9298
1402	0.9018	0.9392		1546	0.8874	0.9286
1405	0.9064	0.9416		1549	0.8857	0.9273
1408	0.9100	0.9435		1552	0.8840	0.9260
1411	0.9128	0.9449		1555	0.8823	0.9247
1414	0.9148	0.9459		1558	0.8808	0.9235
1417	0.9163	0.9467		1561	0.8793	0.9223
1420	0.9176	0.9474		1564	0.8773	0.9210
1423	0.9186	0.9479		1567	0.8752	0.9197
1426	0.9194	0.9484		1570	0.8730	0.9183
1429	0.9201	0.9489		1573	0.8708	0.9169
1432	0.9206	0.9493		1576	0.8686	0.9156
1435	0.9209	0.9496		1579	0.8665	0.9143
1438	0.9213	0.9499		1582	0.8646	0.9130
1441	0.9215	0.9501		1585	0.8626	0.9116
1444	0.9217	0.9502		1588	0.8606	0.9103
1447	0.9218	0.9502		1591	0.8587	0.9090
1450	0.9220	0.9504		1594	0.8569	0.9077
1453	0.9220	0.9504		1597	0.8550	0.9065
1456	0.9220	0.9504		1600	0.8532	0.9053
1459	0.9219	0.9503		1603	0.8515	0.9041
1462	0.9217	0.9501		1606	0.8498	0.9029
1465	0.9213	0.9499		1609	0.8484	0.9018
1468	0.9209	0.9494		1612	0.8470	0.9007
1471	0.9204	0.9489		1615	0.8456	0.8996
1474	0.9198	0.9484		1618	0.8444	0.8986
1477	0.9191	0.9478		1621	0.8433	0.8976
1480	0.9183	0.9473		1624	0.8421	0.8967
1483	0.9174	0.9468		1627	0.8410	0.8960
1486	0.9164	0.9463		1630	0.8399	0.8951
1489	0.9154	0.9458		1633	0.8390	0.8943
1492	0.9143	0.9453		1636	0.8382	0.8937
1495	0.9132	0.9447		1639	0.8376	0.8930
1498	0.9120	0.9440		1642	0.8370	0.8924
1501	0.9107	0.9433		1645	0.8368	0.8919
1504	0.9095	0.9426		1648	0.8368	0.8914
1507	0.9082	0.9419		1651	0.8370	0.8912
1510	0.9068	0.9411		1654	0.8375	0.8911
1513	0.9054	0.9402		1657	0.8383	0.8911

Table D.1 (cont.) Minimum and maximum spectral absorptance of human skin

	Absorptance				Absorptance	
Wavelength (nm)	Minimum	Maximum		Wavelength (nm)	Minimum	Maximum
1660	0.8394	0.8912		1804	0.8825	0.9244
1663	0.8402	0.8915		1807	0.8824	0.9243
1666	0.8413	0.8920		1810	0.8824	0.9243
1669	0.8426	0.8925		1813	0.8823	0.9242
1672	0.8441	0.8932		1816	0.8823	0.9241
1675	0.8459	0.8940		1819	0.8823	0.9242
1678	0.8481	0.8951		1822	0.8824	0.9245
1681	0.8501	0.8964		1825	0.8826	0.9247
1684	0.8518	0.8977		1828	0.8829	0.9249
1687	0.8535	0.8990		1831	0.8834	0.9253
1690	0.8549	0.9003		1834	0.8839	0.9258
1693	0.8563	0.9017		1837	0.8847	0.9264
1696	0.8577	0.9029		1840	0.8857	0.9272
1699	0.8589	0.9041		1843	0.8871	0.9283
1702	0.8601	0.9052		1846	0.8886	0.9294
1705	0.8614	0.9063		1849	0.8906	0.9308
1708	0.8627	0.9075		1852	0.8928	0.9324
1711	0.8640	0.9086		1855	0.8953	0.9342
1714	0.8653	0.9097		1858	0.8985	0.9362
1717	0.8668	0.9107		1861	0.9021	0.9385
1720	0.8682	0.9117		1864	0.9060	0.9410
1723	0.8694	0.9127		1867	0.9104	0.9435
1726	0.8703	0.9133		1870	0.9150	0.9459
1729	0.8710	0.9138		1873	0.9196	0.9484
1732	0.8714	0.9141		1876	0.9236	0.9510
1735	0.8717	0.9144		1879	0.9272	0.9541
1738	0.8720	0.9147		1882	0.9303	0.9567
1741	0.8724	0.9151		1885	0.9328	0.9590
1744	0.8731	0.9159		1888	0.9351	0.9607
1747	0.8738	0.9166		1891	0.9372	0.9621
1750	0.8748	0.9175		1894	0.9388	0.9633
1753	0.8760	0.9185		1897	0.9403	0.9643
1756	0.8771	0.9195		1900	0.9414	0.9650
1759	0.8781	0.9204		1903	0.9424	0.9655
1762	0.8790	0.9211		1906	0.9428	0.9659
1765	0.8797	0.9219		1909	0.9431	0.9662
1768	0.8803	0.9224		1912	0.9434	0.9663
1771	0.8808	0.9227		1915	0.9437	0.9664
1774	0.8812	0.9231		1918	0.9438	0.9665
1777	0.8817	0.9234		1921	0.9439	0.9668
1780	0.8820	0.9238		1924	0.9440	0.9667
1783	0.8822	0.9240		1927	0.9439	0.9666
1786	0.8825	0.9242		1930	0.9438	0.9667
1789	0.8827	0.9244		1933	0.9437	0.9668
1792	0.8828	0.9245		1936	0.9438	0.9668
1795	0.8827	0.9245		1939	0.9439	0.9669
1798	0.8827	0.9245		1942	0.9440	0.9667
1801	0.8826	0.9244		1945	0.9441	0.9667

Table D.1 (cont.) Minimum and maximum spectral absorptance of human skin

	Absorptance				Absorptance	
Wavelength (nm)	Minimum	Maximum		Wavelength (nm)	Minimum	Maximum
1948	0.9442	0.9665		2092	0.9330	0.9565
1951	0.9440	0.9664		2095	0.9326	0.9563
1954	0.9438	0.9663		2098	0.9320	0.9559
1957	0.9439	0.9663		2101	0.9316	0.9556
1960	0.9439	0.9662		2104	0.9313	0.9552
1963	0.9439	0.9661		2107	0.9310	0.9548
1966	0.9439	0.9661		2110	0.9308	0.9544
1969	0.9438	0.9661		2113	0.9305	0.9541
1972	0.9436	0.9661		2116	0.9301	0.9540
1975	0.9434	0.9659		2119	0.9299	0.9536
1978	0.9433	0.9658		2122	0.9298	0.9532
1981	0.9429	0.9656		2125	0.9296	0.9530
1984	0.9426	0.9654		2128	0.9293	0.9527
1987	0.9425	0.9654		2131	0.9293	0.9525
1990	0.9426	0.9653		2134	0.9291	0.9524
1993	0.9427	0.9651		2137	0.9288	0.9523
1996	0.9426	0.9649		2140	0.9288	0.9523
1999	0.9424	0.9646		2143	0.9288	0.9520
2002	0.9422	0.9644		2146	0.9288	0.9520
2005	0.9421	0.9642		2149	0.9287	0.9520
2008	0.9418	0.9642		2152	0.9288	0.9517
2011	0.9416	0.9640		2155	0.9290	0.9518
2014	0.9414	0.9638		2158	0.9289	0.9519
2017	0.9411	0.9636		2161	0.9289	0.9517
2020	0.9408	0.9634		2164	0.9288	0.9516
2023	0.9407	0.9632		2167	0.9289	0.9517
2026	0.9405	0.9630		2170	0.9290	0.9518
2029	0.9403	0.9627		2173	0.9289	0.9515
2032	0.9403	0.9625		2176	0.9289	0.9516
2035	0.9401	0.9624		2179	0.9287	0.9516
2038	0.9399	0.9621		2182	0.9285	0.9514
2041	0.9398	0.9620		2185	0.9284	0.9513
2044	0.9397	0.9618		2188	0.9282	0.9512
2047	0.9395	0.9615		2191	0.9279	0.9509
2050	0.9394	0.9612		2194	0.9276	0.9506
2053	0.9392	0.9610		2197	0.9275	0.9504
2056	0.9388	0.9607		2200	0.9271	0.9503
2059	0.9383	0.9604		2203	0.9268	0.9501
2062	0.9380	0.9602		2206	0.9267	0.9502
2065	0.9374	0.9598		2209	0.9265	0.9501
2068	0.9369	0.9595		2212	0.9265	0.9501
2071	0.9364	0.9591		2215	0.9264	0.9501
2074	0.9359	0.9588		2218	0.9262	0.9499
2077	0.9353	0.9584		2221	0.9261	0.9498
2080	0.9348	0.9581		2224	0.9261	0.9499
2083	0.9343	0.9577		2227	0.9262	0.9499
2086	0.9339	0.9572		2230	0.9262	0.9500
2089	0.9333	0.9568		2233	0.9265	0.9501

Table D.1 (cont.) Minimum and maximum spectral absorptance of human skin

	Absorptance				Absorptance	
Wavelength (nm)	Minimum	Maximum		Wavelength (nm)	Minimum	Maximum
2236	0.9268	0.9502		2371	0.9408	0.9611
2239	0.9272	0.9506		2374	0.9411	0.9613
2242	0.9275	0.9507		2377	0.9412	0.9612
2245	0.9278	0.9509		2380	0.9414	0.9614
2248	0.9281	0.9512		2383	0.9420	0.9621
2251	0.9288	0.9515		2386	0.9422	0.9621
2254	0.9294	0.9518		2389	0.9415	0.9623
2257	0.9297	0.9519		2392	0.9418	0.9625
2260	0.9300	0.9523		2395	0.9421	0.9627
2263	0.9306	0.9525		2398	0.9424	0.9627
2266	0.9311	0.9529		2401	0.9430	0.9633
2269	0.9316	0.9532		2404	0.9433	0.9636
2272	0.9319	0.9535		2407	0.9432	0.9627
2275	0.9321	0.9537		2410	0.9434	0.9627
2278	0.9329	0.9538		2413	0.9440	0.9634
2281	0.9329	0.9543		2416	0.9444	0.9636
2284	0.9330	0.9546		2419	0.9437	0.9640
2287	0.9334	0.9547		2422	0.9444	0.9646
2290	0.9337	0.9550		2425	0.9438	0.9638
2293	0.9341	0.9553		2428	0.9450	0.9648
2296	0.9344	0.9553		2431	0.9453	0.9654
2299	0.9342	0.9554		2434	0.9452	0.9653
2302	0.9344	0.9555		2437	0.9455	0.9661
2305	0.9349	0.9558		2440	0.9462	0.9657
2308	0.9349	0.9563		2443	0.9465	0.9664
2311	0.9354	0.9566		2446	0.9463	0.9654
2314	0.9358	0.9567		2449	0.9467	0.9656
2317	0.9360	0.9564		2452	0.9472	0.9668
2320	0.9359	0.9568		2455	0.9468	0.9661
2323	0.9363	0.9569		2458	0.9465	0.9665
2326	0.9362	0.9574		2461	0.9466	0.9664
2329	0.9367	0.9581		2464	0.9471	0.9668
2332	0.9368	0.9581		2467	0.9470	0.9668
2335	0.9372	0.9581		2470	0.9475	0.9674
2338	0.9376	0.9583		2473	0.9474	0.9667
2341	0.9380	0.9585		2476	0.9483	0.9678
2344	0.9387	0.9589		2479	0.9464	0.9676
2347	0.9390	0.9594		2482	0.9450	0.9668
2350	0.9396	0.9595		2485	0.9487	0.9690
2353	0.9399	0.9597		2488	0.9465	0.9677
2356	0.9396	0.9596		2491	0.9452	0.9698
2359	0.9395	0.9604		2494	0.9470	0.9701
2362	0.9403	0.9605		2497	0.9457	0.9708
2365	0.9405	0.9612		2500	0.9480	0.9771
2368	0.9403	0.9605				